R. & M. No. 3551

MINISTRY OF TECHNOLOGY

AERONAUTICAL RESEARCH COUNCIL
REPORTS AND MEMORANDA

Low-Speed Wind-Tunnel Measurements of Pressure Fluctuations on the Wing of a Twin-Jet Aircraft (Bristol 188)

By J. A. Lawford and A. R. Beauchamp

LIBRARY
ROYAL AIRCRAFT ESTABLISHMENT
BEDFORD.

LONDON: HER MAJESTY'S STATIONERY OFFICE
1968
PRICE 14*s.* 0*d.* NET

Low-Speed Wind-Tunnel Measurements of Pressure Fluctuations on the Wing of a Twin-Jet Aircraft (Bristol 188)

By J. A. Lawford and A. R. Beauchamp

Reports and Memoranda No. 3551*
December, 1966

Summary.

Root-mean-square intensities and spectra of local pressure fluctuations were measured by transducers at two positions on the inner part of the wing and four on the outer part, while low-frequency pressure fluctuations on the upper surface were obtained at a further fifteen positions on the outboard part of the wing by a 'creeper' and transducer.

The low-frequency component of pressure and load fluctuations increases in intensity with increasing incidence; on the inboard wing this increase is fairly abrupt and is associated with a change in the form of the mean flow field about the wing; on the outer wing the intensity increases more gradually with incidence.

Buffet boundaries have been assessed tentatively from the incidence associated with rapid rise of load fluctuation on the inner wing; more severe limitations could however be imposed by conditions on the outer wing, where likely buffeting excitation is more difficult to assess.

Leading-edge strakes may modify the buffet boundaries, giving a gain of about 0·2 in usable C_L trimmed. There is some evidence that leading-edge droop would considerably reduce load fluctuations.

CONTENTS

*Replaces R.A.E. Tech. Report 66 399—A.R.C. 29 230.

---

1. *Introduction.*

The work described in this Report formed part of a more general investigation into the aerodynamic origins of buffeting. It had two main objectives; to add to the data already accumulated on the relation between the time-dependent and the mean-flow properties of unsteady flows commonly occurring in aeronautics, and to provide a tentative estimate of the buffet boundary for a particular aircraft (the Bristol 188) at low Mach number. The investigation was confined to the flow over the wing, and included a study of the effects of some leading-edge devices which were expected to delay the onset of buffeting.

Detailed measurements were made of the intensities and spectra of the local fluctuating loads at a number of points on the wing, for several configurations and attitudes of the model. These were supplemented by a study of the mean flow field using the surface oil flow method, and (in some cases) by measurement of the mean static pressure near the trailing-edge of the inner wing. A test was also made with the model oscillating in pitch, to demonstrate the lack of coupling between the random fluctuating loads and those due to the oscillatory motion, and so to give some justification for confining the bulk of the measurements to a rigid model.

Interpretation of the data thus accumulated depends upon several observations outside the scope of the present experiments. It must be recognised, firstly, that buffeting is a forced oscillation of some vibrational mode of the aircraft structure; by definition, there is no reinforcement of the forcing field due to the vibrational motion. This is the essential distinction between buffeting and flutter, which justifies a separate study of the unsteady loads experienced by a rigid model. However, it also introduces some uncertainty into the interpretation of the results. In principle, if the fluctuating pressure field were known in sufficient detail (which would involve knowledge of the two-point correlation over the entire wing surface), it would be possible to derive the oscillatory motion of the wing in any mode, given the aerodynamic damping and vibrational characteristics of the structure in that mode. But, quite apart from the prohibitive effort involved in describing the forcing field for this purpose, there would ultimately be no clear indication of the point at which buffeting could be said to begin. No critical change, analagous

to divergence in flutter, could be expected in the properties of the motion. Instead, it would be necessary to define some threshold level of vibration beyond which buffeting becomes intolerable. Evidently the choice of this level would be to some extent arbitrary, and might well depend, among other things, upon the particular mode of vibration excited.

However, there is reason to suppose that the onset of buffeting requires a major change in the structure of the flow as well as a quantitative change in the properties of the exciting field. Observed buffeting frequencies are usually low (of the order of 10 cycles per sec), being associated with a fundamental mode of vibration of one or other of the major aircraft components. This implies the presence of a relatively large-scale unsteadiness in the forcing field; it suggests, in particular, that if a fundamental vibration of the wing structure is to be excited by the flow round it, a significant departure from attached or streamline flow must first occur. It suggests, also, that a spectral analysis of the local loads might be more revealing than measurements of total intensity and, since a substantial level of low frequency fluctuation is likely to imply relatively high correlation over the wing surface, that extensive measurements of correlations might be avoided.

It is consequently supposed here that there is a risk of buffet whenever there is evidence of a substantial increase in level of local low-frequency load fluctuations compared with the zero-incidence datum level, together with a large-scale change in the flow structure. Under these conditions the high-level fluctuations are likely to extend over a considerable area and to be sufficiently well correlated to generate substantial loads in some natural mode of vibration of the structure.

2. *Methods of Measurement.*

The equipment used for the measurements was similar to that of Ref. 1. The pressure transducer, of the capacity type, was reduced in size compared with that of Ref. 1, and the casing modified to give a flush fitting in both wing surfaces (*see* Fig. 3). Two transducers were fitted on the inner wing, and four on the outer wing, as shown in Fig. 1. Additional measurements were made on the outer wing using a creeper consisting of a $\frac{1}{4}$ inch square flat plate, 0·06 inch thick with a 0·024 inch diameter hole in the centre of one surface, connected by 17 inches of 1 mm metal tubing to a transducer inside the nacelle, so that the creeper could be placed at any required position on the outer wing upper surface. Since the length of tubing between creeper and transducer caused a frequency-dependent attenuation of the pressure fluctuations at the transducer, the creeper could be used only to measure low-frequency fluctuations where attenuation was small, of known magnitude, and therefore open to correction. It was calibrated by comparison with results obtained from the fixed transducers (at positions A and B in Fig. 1).

The transducers at fixed positions in the wing were used principally to measure the fluctuations in the pressure difference between the orifices on the upper and lower surfaces—that is, fluctuations in the local load at the transducer. Pressure fluctuations on either surface separately could be obtained by connecting the transducer orifice on the opposite surface to atmosphere outside the tunnel by a rigid-walled pipe.

A block diagram of the apparatus is shown in Fig. 2. The output from the transducer passed through a Southern Instruments oscillator and demodulator to an amplifier. Parallel outputs from this amplifier were taken to a thermojunction whose d.c. output was read on a galvanometer, and also, *via* a logarithmic potentiometer, to a Muirhead Pametrada wave analyser, with low frequency modulator giving a frequency range from 2 to 20 000 cycles per sec. The analyser output was connected to a second thermo-junction and galvanometer. By means of a switch the output of the Southern Instruments demodulator could be replaced at the amplifier input by a calibrating signal of any required frequency and rms voltage from an oscillator and microvolter.

3. *Details of Model and Tests.*

The 1/10th scale model of the Bristol 188 aircraft was as shown in Fig. 1 and main dimensions are tabulated in Table 1. The wing had a 4 per cent thick bi-convex section, with sharp leading-edge and finite trailing-edge thickness (0·004c). Pressure transducers were fitted at the positions shown. The tests were made in the No. 2 $11\frac{1}{2}$ ft × $8\frac{1}{2}$ ft wind-tunnel at the R.A.E., using a wind speed of 150 ft/sec except

where otherwise stated ($R = 1{\cdot}16 \times 10^6$ based on aerodynamic mean chord $\bar{c}$). For some of the tests leading-edge strakes were fitted as shown in Fig. 1. (These are strakes No. 1 of Ref. 2). The model was mounted on struts at the wing lower surface and wires at the tail.

The following tests were made:

(a) *Flaps* 0°. *No leading-edge strakes.* Tests on inner wing only:

Local load fluctuations at 0·5*c* and 0·85*c*. Rms intensities and frequency spectra over incidence range 0° to 16°. Brief measurements at 280 ft/sec to check the effect of change of wind speed.

Fluctuation of pressure on upper and lower surfaces separately, at 0·85*c*. Rms intensity over the incidence range, and spectra at $\alpha = 14{\cdot}2°$.

Fluctuation in local load at 0·5*c* and 0·85*c*, with the model oscillating ± 1 deg about a mean incidence of 10·1°.

(b) *Flaps* 50°. *No leading-edge strakes.* Tests on inner wing only:

Fluctuations in local load. At 0·5*c*, rms intensities and spectra over the incidence range; at 0·85*c*, rms intensities and the low frequency end of spectra over the incidence range.

(c) *Flaps* 0°. *Leading-edge strakes on.* Tests on inner wing only:

Local load fluctuations at 0·5*c* and 0·85*c*. Rms intensities and frequency spectra over the incidence range. At 0·85*c* rms intensities over the incidence range at 280 ft/sec, with a spectrum at $\alpha = 12{\cdot}2°$.

(d) *Flaps* 50°. *Leading-edge strakes on.*

On the inner wing, fluctuations in local load; rms intensities over the incidence range at 0·5*c* and 0·85*c*, with spectra at 0·5*c* and the low frequency end of spectra at 0·85*c*.

On the outer wing, rms intensities and spectra of load fluctuations at the four transducer positions over the incidence range 0° to 16°. Measurements of pressure fluctuations at the low frequency end of the spectrum using the creeper at nineteen positions on the upper surface, over an incidence range from 2° to 12°.

Surface oil flow patterns at incidences from 0° to 16° were obtained on the outer wing.

(e) *Flaps* 0°. *No leading-edge strakes. Leading-edge of wing drooped* 25° *from* 0·1*c*.

Rms intensities of local load fluctuations were measured at 0·85*c* on the inner wing, over the incidence range 0° to 14°.

4. *Surface Flow Patterns.*

Surface flow patterns over the whole wing, obtained using oil and titanium oxide mixture, have already been given in Ref. 2. Photographs of flow patterns on the outer wing only, obtained using a mixture of paraffin oil and anthracene, are given here in Fig. 22. These photographs were taken by ultra-violet light, in which anthracene is fluorescent.

Fig. 4 shows sketches of the patterns on the inner wing at about 8° incidence, in the datum condition and also with flaps down and strakes on. The pattern in the datum condition (Fig. 4a) indicates that the flow was essentially two-dimensional in character, with an attachment line parallel to the leading-edge at about 0·5*c*. This line represents the closure of a 'bubble'[3], which lies between the leading edge and the attachment line. Fig. 5 shows the variation in the length of this inner wing bubble with incidence, deduced from surface patterns. The surface of separation from the leading edge did not appear to reattach at incidences greater than $10\frac{1}{2}°$: this is roughly consistent with the divergence of the static pressure at 0·97*c* on the inner wing upper surface, shown in Fig. 6 to occur at an incidence of about $9\frac{1}{2}°$.

When the flaps were at 50°, the bubble length at low incidence differed only slightly from that with flaps at 0°, but as incidence increased above 9°, the rearward movement of the reattachment was slower than at flaps 0°, and it did not reach the flap hinge until the incidence was about 13°. The surface pattern at incidences up to 9° was not greatly affected by the flap, but there was some increase of inflow over the nacelle and the demarcation line between streamlines originating at the body and at the nacelle was moved slightly inboard.

The fitting of leading-edge strakes (Fig. 4b) makes the inner wing flow pattern more three-dimensional in nature, vortices being shed from the oblique edges of the strakes at all incidences other than zero. The attachment line was no longer parallel to the leading edge, the bubble being almost entirely eliminated in the junctions and reduced in extent at the centre of the wing panel.

On the outer wing (Fig. 22), the pattern appeared at high incidence (12° and over) to resemble that on a delta wing with about 45° of leading-edge sweep, but at moderate incidences it was modified by the kink in the leading edge. At $\alpha = 4°$ there appeared to be two distinct vortices associated with the two parts of the leading edge on either side of the kink. At $\alpha = 6°$ the vortex from the edge inboard of the kink appeared to have spread across the aileron horn and the vortex from the more highly swept edge outboard of the kink was confined to a small region near that edge. At $\alpha = 8°$ the flow resembled that for a delta wing, but with some complication near the highly swept edge. As incidence increased this region became smaller and apparently had disappeared entirely by $\alpha = 12°$.

5. *Results.*

5.1. *Presentation and Interpretation of Results.*

The rms intensities p of the pressure or local load fluctuations are divided by q ($= \frac{1}{2}\rho V^2$) and plotted against incidence. The frequency spectra are given as plots of $\sqrt{nF(n)}$ against $\log n$; Owen has shown[5] that the aerodynamic excitation within the narrow acceptance band associated with vibration in any particular mode of the structure is proportional to $\sqrt{nF(n)}$, and since

$$\left(\frac{p}{q}\right)^2 = \int_{n=0}^{n=\infty} nF(n)\, d\,(\log n)$$

an integrable power spectrum can be obtained by squaring the ordinates.

From the spectra or, in some cases, from two or three measurements at the low frequency end of the spectrum, a 'low frequency component' of the pressure or load fluctuation is obtained and plotted against incidence. This low frequency component is arbitrarily defined as the value of $\sqrt{nF(n)}$ at $n = 0{\cdot}2$. This corresponds to 4·8 cycles/sec for the full-scale aircraft at 175 kt, which is close to likely frequencies for structural vibration at the estimated approach speed. This value of n therefore represents the order of frequency likely to cause buffeting. The form of the spectra however is such that interpretation of the results would not be greatly different if another value of n between 0·1 and 0·3 had been chosen.

Since buffeting depends upon the structural as well as the aerodynamic characteristics of an aircraft, its probability cannot be entirely assessed from measurements of low-frequency excitation. However, in making tentative estimates of buffet boundaries it may be helpful to bear in mind that levels of 0·04 in $\sqrt{nF(n)}$ are regarded, from past experience, as high. They have usually been found to be associated with large-scale unsteady flows like those occurring behind dive brakes[1] and on the rear bulkheads of bomb bays[4]. On the other hand, levels of less than 0·005 correspond more to fluctuation levels in turbulent boundary layers. As a rough guide, it seems reasonable to assume that conditions conducive to buffeting are becoming established when $[\sqrt{nF(n)}]_{n=0\cdot2}$ has reached some value between 0·005 and 0·04, and in this Report an arbitrary value of 0·01 has been taken for this purpose. The rate of increase in low frequency component with incidence must affect the dependability of this assessment: if, as on the inner wing and the outer wing near the nacelle, the low frequency component remains at a low level until a critical incidence is reached and then rises steeply, the estimated limiting incidence is insensitive to the value of limiting low frequency component selected, and there is a clear risk of buffeting at incidences outside the boundary: if, as on the outboard part of the outer wing, the low-frequency component rises slowly over a large incidence range, the situation is more difficult to assess and estimated buffet boundaries must be treated with more reserve.

The pressure fluctuation measurements obtained for each configuration will now be discussed.

5.2. *Flaps* 0°. *No L.E. Strakes* (*Figs.* 7 *to* 10).

The results obtained from transducers at 0·5*c* and 0·85*c* on the inner wing show that although the rms load fluctuation increased rapidly with increase of incidence above about 4°, the low-frequency component did not rise appreciably until an incidence between 6° and 7° was reached. The highest levels of both rms fluctuation and of low-frequency component were in the region 10° to 12°—that is, they reached a maximum when the surface of separation from the leading edge no longer reattached forward of the trailing edge. The low-frequency component reached a value of 0·01, and was rising rapidly, at incidences of 6·4° and 7·9° for 0·5*c* and 0·85*c* respectively, corresponding to values of C_L trimmed of 0·36 and 0·465 (Ref. 2).

Fig. 9 shows the small effect due to a change of wind speed from 150 ft/sec to 280 ft/sec.

Fig. 10 shows the pressure fluctuations on each surface of the wing separately. It is noticeable that the fluctuations on the lower surface began to increase at about the incidence at which low-frequency fluctuations appear in the local loading. This is regarded as evidence in support of the hypothesis that the increase in low-frequency component coincided with a change in mean flow over the whole wing. The increased pressure fluctuations on the lower surface were mainly at low frequencies (Fig. 10b).

5.3. *Flaps* 50°. *No L.E. Strakes* (*Figs.* 11 *and* 12).

The results on the inner wing at 0·5*c* and 0·85*c* show similar behaviour to that with flaps 0°, but at 0·5*c* both the rms intensity and the low frequency component of the load fluctuations rose at a smaller incidence. The low frequency component reached a value of 0·01 at $\alpha = 5{\cdot}1°$, but this corresponds to a higher value of C_L trimmed than for zero flap angle, *viz* 0·52 (Ref. 2).

The measurements at 0·85*c* were on the surfaces of the deflected flap. The upper surface flow would separate from the flap hinge, and the lower surface flow from the trailing edge, so the upper surface of the transducer was inside a separation bubble which would include a pair of highly unsteady standing eddies[3]. There was therefore a higher level of load fluctuation at this position at low incidence than occurred with flaps 0°, the low frequency component being above 0·01 throughout the incidence range (apart from incidences close to 6°, where it was equal to 0·01). But a value of low frequency component of 0·015, confined only to a small area of the flap, is probably unimportant, and in any event flaps down 50° is an unlikely flight configuration at low incidence.

5.4. *Flaps* 0°. *L.E. Strakes on* (*Figs.* 13 *to* 15).

Comparison of Fig. 13 with Fig. 7 and Fig. 14 with Fig. 8 shows that the strakes gave a large increase in the incidence at which the low frequency component rose, and some improvement in the rms intensities.

At 0·5*c* the incidence for $[\sqrt{nF(n)}]_{n=0{\cdot}2} = 0{\cdot}01$ increased from 6·4° to 9·6° (0·36 to 0·55 in C_L trimmed). At 0·85*c* the increase was from 7·9° to 10·8° (0·46 to 0·62 in C_L trimmed). The spectra at 0·5*c* were measured after a break in the tests during which the strakes were removed and replaced, and lower rms intensities were obtained at some incidences while measuring the spectra than during the earlier tests. This was probably due to slight differences in the fit of the strakes. The measurements at 0·85*c* were all made before the break in the tests, so no difference would be expected.

5.5. *Flaps* 50°. *L.E. Strakes on.*

(i) *Inner wing* (*Figs.* 16 *and* 17).

The strakes again gave a large improvement in the incidence for rapid increase of low-frequency fluctuations, and some decrease in rms intensity. (Compare Fig. 16 with 11, and 17 with 12). At 0·5*c* $[\sqrt{nF(n)}]_{n=0{\cdot}2} = 0{\cdot}01$ at $\alpha = 8{\cdot}2°$ (C_L trimmed 0·69) compared with $\alpha = 5{\cdot}1$ (C_L trimmed 0·51) without strakes. At 0·85*c*, $[\sqrt{nF(n)}]_{n=0{\cdot}2}$ lay below 0·01 between $\alpha = 5{\cdot}2°$ and $\alpha = 9°$ (C_L trimmed between 0·5 and 0·74); as noted in Section 5.3, the higher values of low frequency component at low incidence are probably of little practical importance.

(ii) *Outer wing* (*Figs.* 18 *to* 24).

The surface flow patterns and low-frequency component contour diagrams (Figs. 22 and 23) indicate that the maximum low-frequency component lay under the vortex in a predominantly vortex flow. But low-frequency fluctuations were more widely spread over the wing when the flow became more of the 'bubble' type, as it did at the higher incidences. The mean value of the low-frequency component (Fig. 24) rose fairly smoothly with increase of incidence up to 12°, although the form of the flow pattern varied widely in this range.

The following Table shows the incidences and values of C_L trimmed at which the low-frequency component of load fluctuation reached 0·01 at each of the four transducer positions on the outer wing; corresponding values are also given for the mean upper-surface pressure fluctuation over the whole outer wing from the creeper results.

Position	$\alpha°$	C_L trimmed
A	8·9	0·77
B	4·1	0·43
C	11·1	0·87
D	6·4	0·57
Mean	6·45	0·58

But since the level of 0·01 is not always associated with a rapidly increasing intensity of fluctuation with incidence—in particular over the extreme outer part of the wing—it is now a much less convincing guide to conditions conducive to buffeting. For example, although the level at position B rises to 0·01 at $\alpha = 4{\cdot}1°$, as indicated in the Table, it is still less than 0·015 at $\alpha = 8°$.

5.6. *Flaps* 0°. *No L.E. Strakes. L.E. Droop on Inner Wing* 25° (*Fig.* 25).

A few measurements of rms load fluctuations were made at this condition with the transducer at 0·85c on the inner wing. Fig. 25 shows that the fluctuations remained at a low level up to an incidence of 14°. Without leading-edge droop, leading-edge separation occurs at all incidences other than zero, the reattachment line moving back with increase of incidence until reattachment no longer occurs. With leading-edge droop the incidence at which leading-edge separation first occurs is greater than zero, and provided, as is likely, that the rate of movement of the reattachment line with incidence is substantially unaltered, the incidence at which reattachment ceases to occur will be similarly increased. Measurement of lift with drooped leading edge are available only with trailing-edge flaps at 50° (Ref. 2, Fig. 21). The droop causes a loss in C_L trimmed which increases with incidence to a maximum of about 0·16 at $\alpha = 11°$. It appears likely that the risk of buffeting due to load fluctuations on the inner wing could be delayed by about 6° of incidence by leading-edge droop; if a similar improvement were achieved on the outer wing, a substantial improvement in maximum usable lift could probably be obtained.

5.7. *General Discussion of Pressure Fluctuation Results.*

The results indicate a rapid rise in level of the low frequency component of the local fluctuating loads on the inner wing as the flow changes from one with separation from the leading edge accompanied by reattachment further aft on the wing surface to a fully separated flow of the bluff-body type. This is believed to be conducive to buffeting. Although the rise in level does not occur at precisely the same incidence everywhere on the inner wing, the differences are small and a level of 0·01 at 0·5c is probably a reasonable guide to the possible buffet boundaries for the configurations tested. These are summarised in the following table:

Configuration	$\alpha°$	C_L trimmed
Flaps 0°. No strakes	6·4	0·35
Flaps 0°. Strakes on	9·6	0·56
Flaps 50°. No strakes	5·1	0·51
Flaps 50°. Strakes on	8·2	0·69

The outer wing presents a more difficult problem of interpretation. While the behaviour at points like A and C, at the inboard end of the outer wing, where the leading-edge sweep is least, is qualitatively the same as on the inner wing, and can presumably be given the same interpretation, the behaviour characteristic of points like B and D on the outboard part of the outer wing is noticeably different. Here, although the level of 0·01 in low-frequency component may be reached at fairly low incidence, the associated rate of rise is much less than before, and the arbitrarily chosen 0·01 is consequently a much less convincing guide to the possible buffet boundary. Moreover, it is evident that the early rise in level is here associated with a vortex flow over the outer part of the wing, and therefore with a fluctuating pressure field that probably differs markedly in character from the more two-dimensional field on the inner wing. It may therefore be wise to disregard these outermost observations in the first instance, and to take the measurements at the position A as the guide to the buffet boundary for the outer wing. This suggests a limiting incidence of 8·9°, and a corresponding C_L trimmed of 0·77 for the flaps 50°, strakes on configuration. However, it would be well to bear in mind that a more severe limitation may in fact be implied, the probable lower limit being given by the mean fluctuation on the outer wing as $\alpha = 6{\cdot}45°$, C_L trimmed = 0·58.

5.8. *Model Oscillating in Pitch* (*Fig.* 26).

These tests were made to find whether an oscillation of the aircraft, possibly initiated by the measured excitation in the static condition, would cause much modification of the excitation itself. The model was oscillated about a mean incidence of 10·1°, with an amplitude of ± 1 deg, at a frequency of 7·5 cycles/sec ($n = 0{\cdot}062$), this being the highest frequency possible at this amplitude without overstressing the model. The tests were made with flaps 0°, without strakes. A correction for inertia effects on the transducers was made by subtracting from the square of the analyser output the square of the corresponding output while oscillating the model with the wind off.

The results show a peak reading at the oscillation frequency, but no very great change in the random fluctuations at other frequencies. There is some reduction in the fluctuations at frequencies below $n = 1$ at $x/c = 0{\cdot}85$, up to about 50% reduction at the lowest frequencies, but this occurs with a forced oscillation of very large amplitude, and it is probable that apart from the peak at the oscillation frequency, oscillation in pitch will have little effect on load fluctuations. The values of $\sqrt{nF(n)}$ at the oscillation frequency are equivalent to a slope of the pressure difference *vs* incidence curve of about one third of the value under static conditions.

6. *Conclusions.*

The low frequency component of the fluctuating local load on the inner wing increases rapidly above a certain value of incidence, and this is believed to indicate a greatly increased risk of buffeting. This increase is associated with a change in mean flow from leading-edge separation accompanied by reattachment to the wing surface to a fully separated flow. The rms load fluctuations and the low-frequency component both reach a maximum when the main flow ceases to reattach to the wing upper surface forward of the trailing edge. The load fluctuations are much relieved if the leading-edge is drooped by 25° over the first 10 per cent of the chord.

The following tentative buffet boundaries have been estimated for the configurations tested from consideration of the fluctuating loads on the inner wing.

Configuration	$\alpha°$	C_L *trimmed*
Flaps 0°. No strakes	6·4	0·35
Flaps 0°. Strakes on	9·6	0·56
Flaps 50°. No strakes	5·1	0·51
Flaps 50°. Strakes on	8·2	0·69

Buffeting excitation on the outer wing was more difficult to assess and buffet boundaries have not been deduced from these results. However buffeting could well be initiated on the outer wing, in some configurations at least, at incidences lower than those given for the inner wing.

Negligible coupling was observed between oscillation in pitch and the random forcing field.

7. *Comparison with Observations on the Bristol* 188 *Aircraft in Flight.*

Brief observations of buffeting behaviour were made on the Bristol 188 aircraft during flight tests (reported in an unpublished Bristol Aircraft Company paper in 1963). Most of these were made with lowered undercarriage, and direct comparison with the results of this report is possible only for the case of flaps at 0° with strakes on, for which tunnel measurements were confined to the inner wing. The flight observations in this case were as follows:

Airspeed (*kts*)	C_L	α (*from Ref.* 2)	*Observation*
202	0·59	10·6°	Mild low-frequency buffet
180	0·74	13·2°	Rear-end buffet
165	0·88	18°	Buffeting

Except for buffet very close to the estimated stalling speed, the intensity of buffet was not such as to discourage flight under the conditions where it occurred.

The observed onset of buffeting agrees well with the estimate of $C_L = 0{\cdot}56$ from the tunnel measurements. It is notable also that buffeting intensity remained at an acceptable level at incidences giving a low-frequency component of load fluctuation on the inner wing of between 0·03 and 0·04, and at which it appears likely (from the measurements with flaps at 50°) that fluctuations on the outer wing were at a similar level. However in interpreting the flight results the reduced dynamic pressure at high C_L should be borne in mind.

The incidences at which the first two flight observations were made are indicated on Figs. 13 and 14.

LIST OF SYMBOLS

p	Root mean square pressure or local load fluctuation
f	Frequency, cycles per sec
V	Free stream velocity
c	Local chord
$\bar{c}$	Aerodynamic mean chord
n	Frequency parameter $\left(= \frac{f\bar{c}}{V} \right)$
$F(n)$	Spectrum function, such that $F(n)\ \delta n$ is the contribution to $(p/q)^2$ of frequencies between n and $n+\delta n$ (Ref. 5)

REFERENCES

No.	*Author(s)*	*Title, etc.*
1	T. B. Owen	Low speed static and fluctuating pressure distributions on a cylindrical body with a square flat-plate air brake. ARC CP 288. January 1956.
2	J. W. Leathers	Low speed wind-tunnel tests on a 1/10th scale model of a twin jet aircraft, Bristol 188. R.A.E. Tech. Note Aero 2515. July 1957. ARC 20047.
3	E. C. Maskell	Flow separation in three dimensions. R.A.E. Report Aero 2565. November 1955. ARC 18063.
4	R. Fail, T. B. Owen and R. C. W. Eyre ..	Low speed wind-tunnel tests on the flow in bomb bays and its effect on drag and vibration. R.A.E. Report Aero 2511. May 1954. ARC 17412.
5	T. B. Owen	Techniques of pressure-fluctuation measurements employed in the R.A.E. low-speed wind tunnels. AGARD Report 172. March 1958.

TABLE 1

Details of Model

Scale – 1/10th

Wing	
Area	3·96 sq. ft.
Span	3·508 ft.
Aspect ratio	3·11
Root chord	1·425 ft.
Tip chord	0·183 ft.
Dihedral	0°
Wing-body angle	2°
Section:	
Root to 52% semispan. Bi-convex, sharp L.E. $t/c = 0{\cdot}04$. 52% semispan to tip. Graded from above section to R.A.E. 104, $t/c = 0{\cdot}078$.	
Leading-edge sweepback:	
Inboard of nacelles	0°
Outboard of nacelles, to 52% semispan	38°
52% semispan to tip	64°
Wing strakes	
Total area of strakes	0·030 sq. ft.
Max. chord	0·15 ft.
L.E. spanwise dimension	0·025 ft.
T.E. spanwise dimension	0·075 ft.
Trailing-edge flaps (inboard of nacelles)	
Total area aft of hinge line	0·249 sq. ft.
Total span	0·713 ft.
Hinge-line position	0·75*c*
Fuselage	
Length	7·03 ft.
Max. width	0·380 ft.
Max. height	0·496 ft.
Distance from nose to wing L.E.	2·935 ft.
Nacelles	
Length	3·092 ft.
Max. external diameter	0·367 ft.
Angle of nacelle datum to wing datum	−2°
Distance from nose to wing L.E.	1·08 ft.

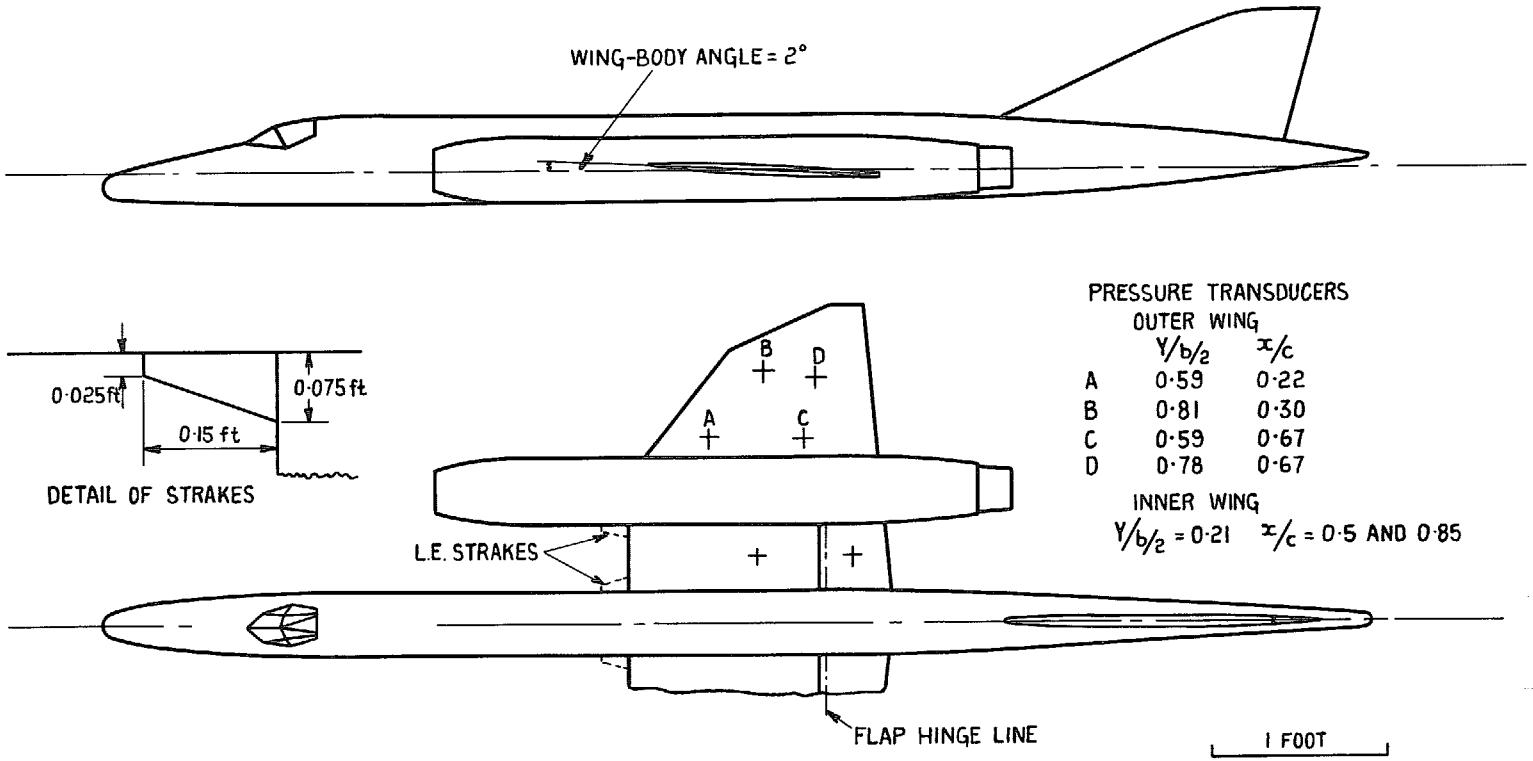

FIG. 1. Bristol 188 1/10th scale model general arrangement.

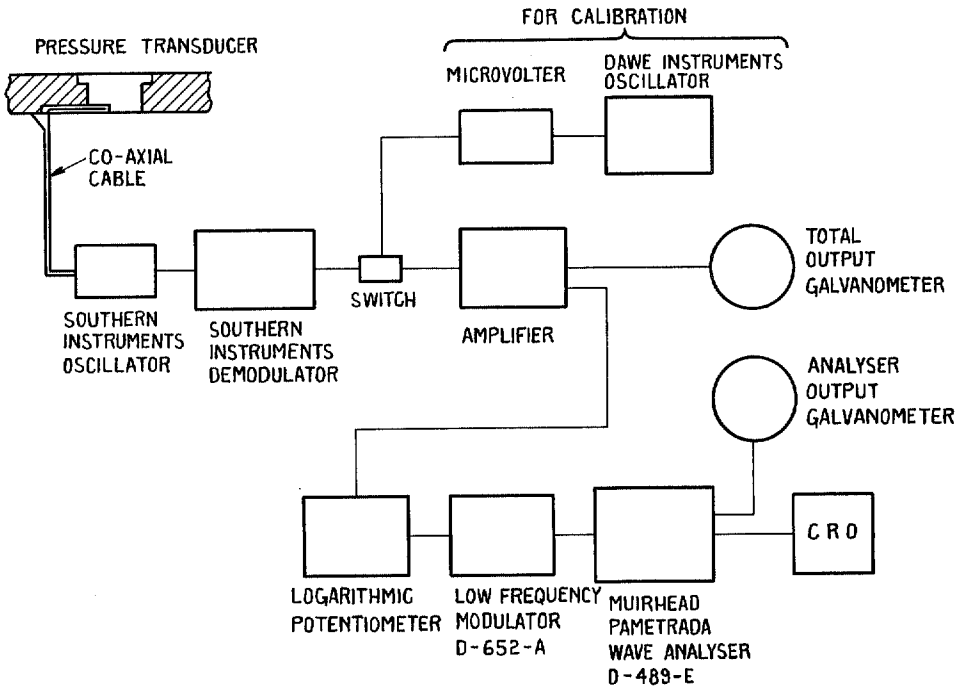

FIG. 2. General arrangement of apparatus for measurement of pressure fluctuations.

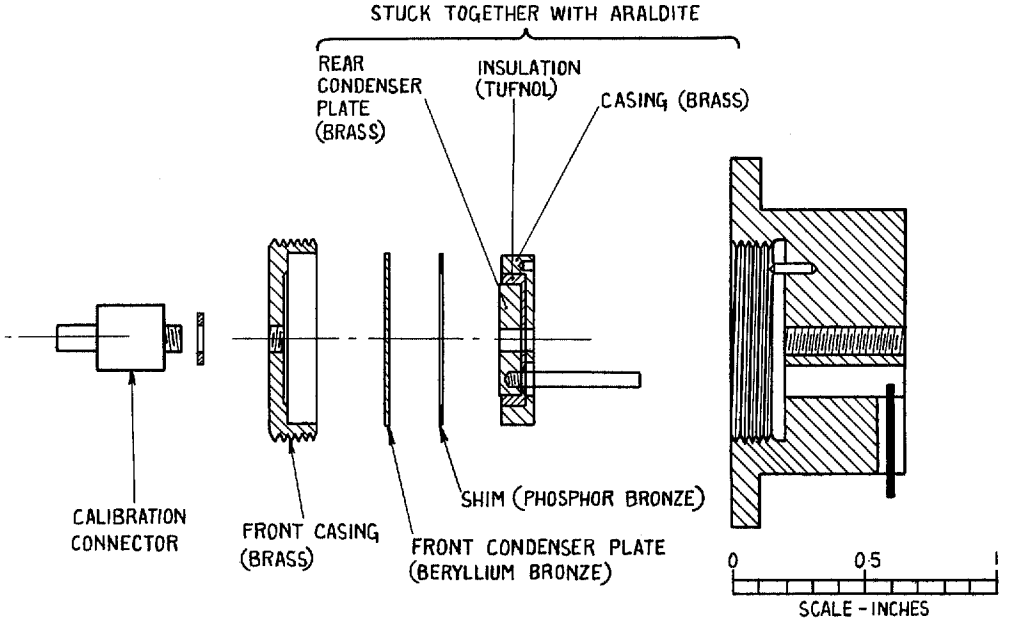

FIG. 3. Exploded section of capacity type pressure transducer.

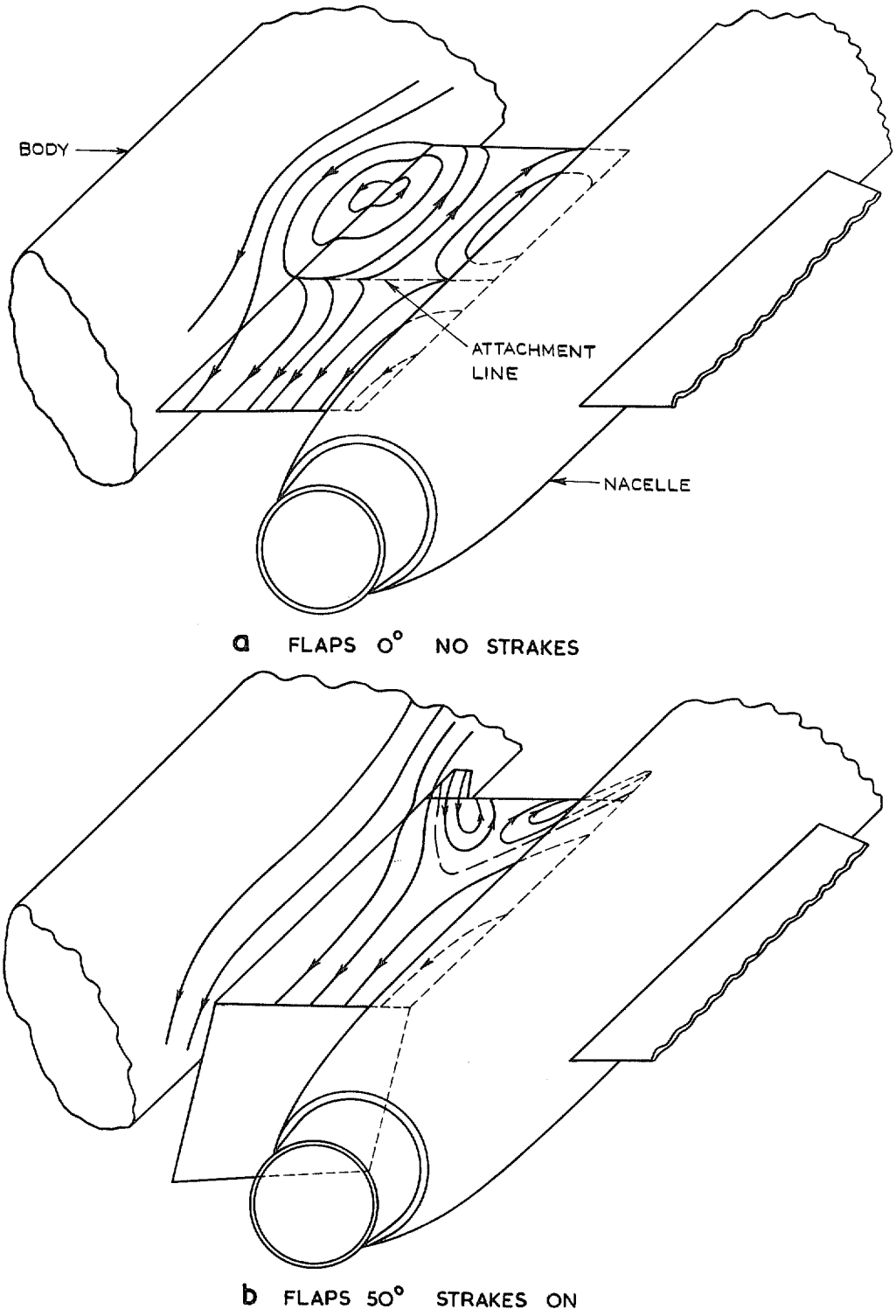

FIG. 4 a and b. Surface flow patterns on inner wing, $\alpha = 8°$ approx.

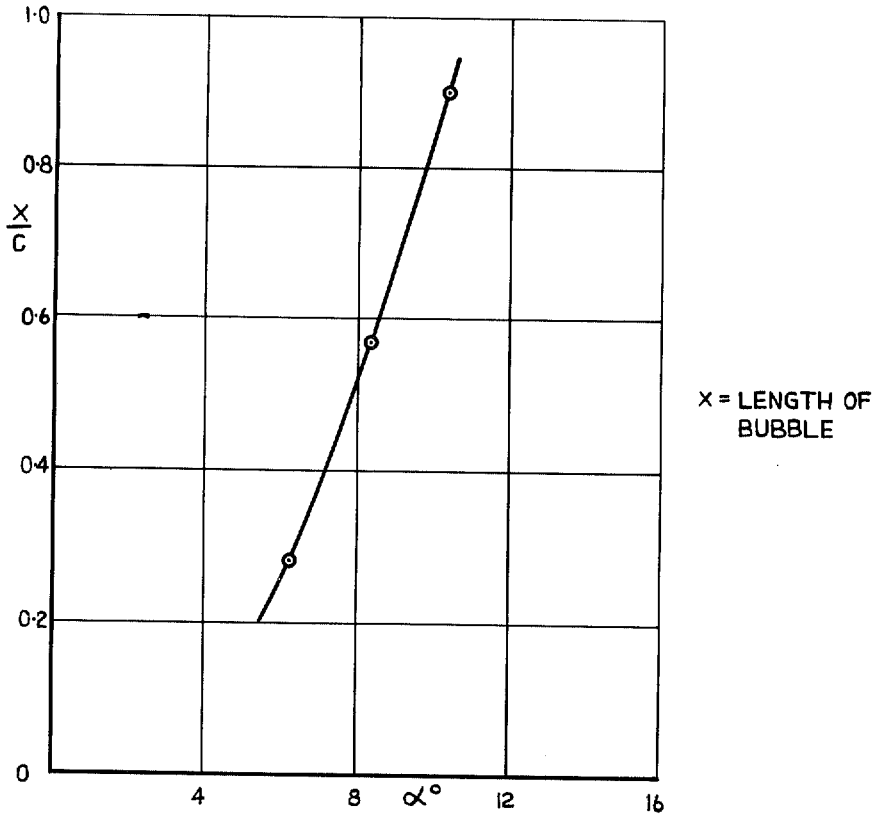

FIG. 5. Variation of bubble length with incidence. Flaps 0°, $V = 150$ ft/sec, no strakes.

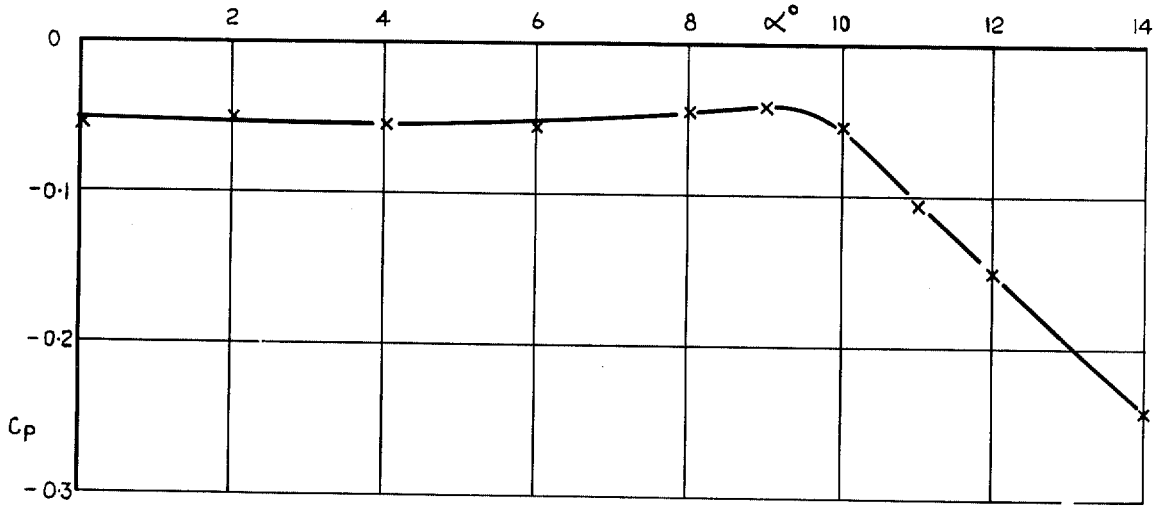

FIG. 6. Static pressures at 0·97c on upper surface of inner wing. Flaps 0°, no strakes, $V = 150$ ft/sec.

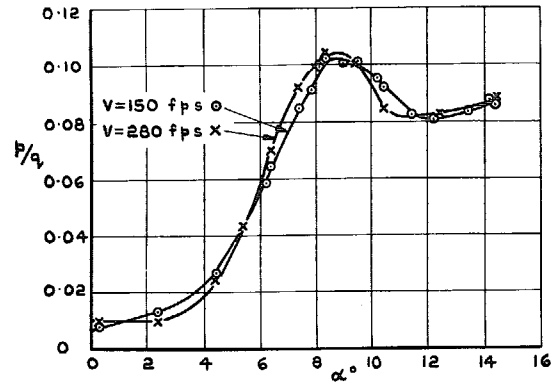

a rms LOAD FLUCTUATION

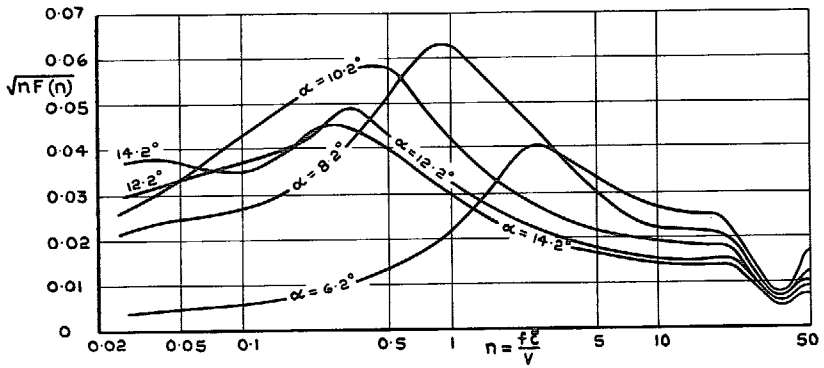

b SPECTRA OF LOAD FLUCTUATION V=150 ft/sec

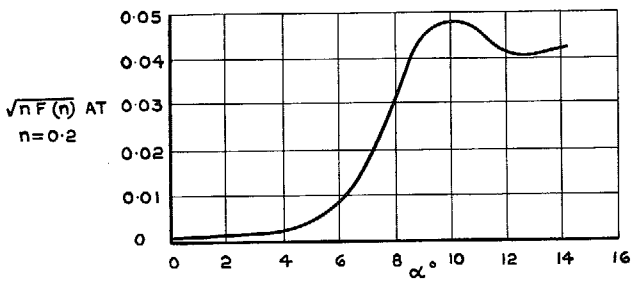

c "LOW FREQUENCY COMPONENT" OF LOAD FLUCTUATION V=150 ft/sec

FIG. 7 a – c. Local load fluctuations at 0·5c on inner wing. Flaps 0°, no strakes.

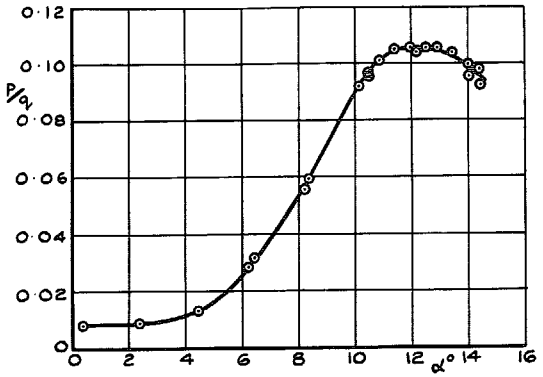

a rms LOAD FLUCTUATION

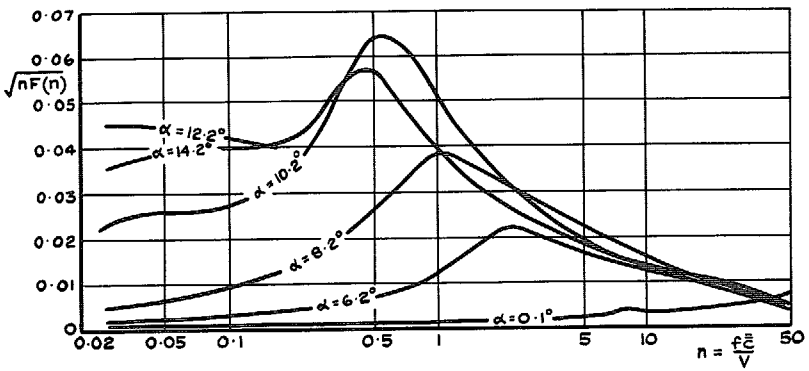

b SPECTRA OF LOAD FLUCTUATION

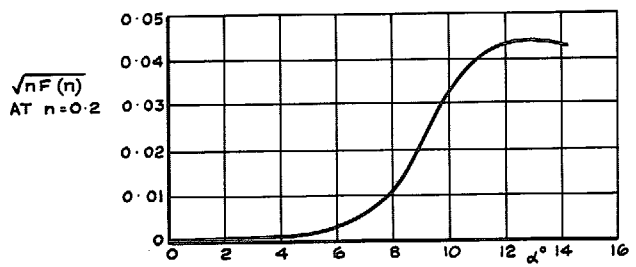

c "LOW FREQUENCY COMPONENT" OF LOAD FLUCTUATION

FIG. 8 a – c. Local load fluctuations at 0·85c on inner wing. Flaps 0°, no strakes, V = 150 ft/sec.

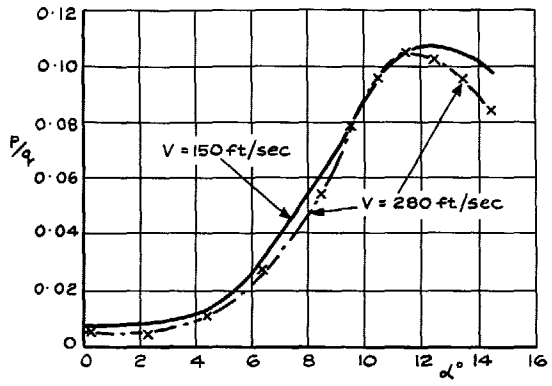

a rms LOAD FLUCTUATION

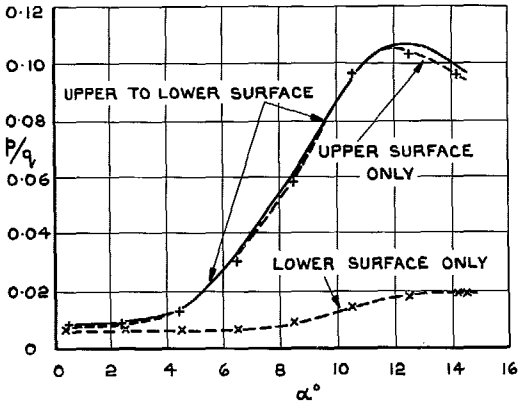

a rms PRESSURE FLUCTUATION

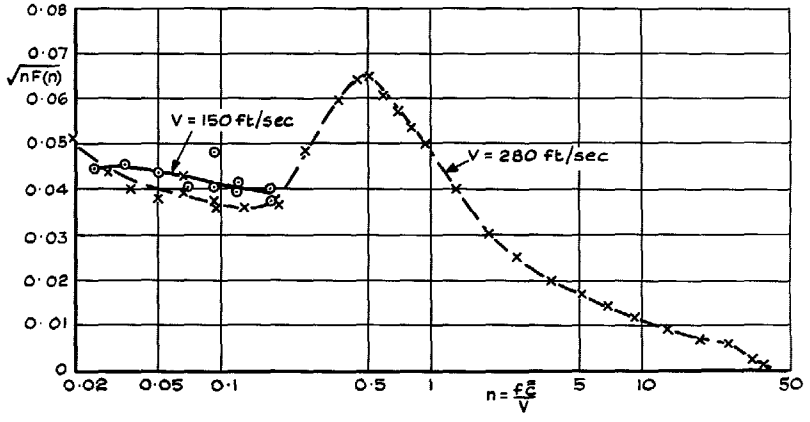

b SPECTRA OF LOAD FLUCTUATION $\alpha = 12{\cdot}2°$

FIG. 9 a and b. Effect of wing speed on local load fluctuations at 0·85c on inner wing. Flaps 0°, no strakes.

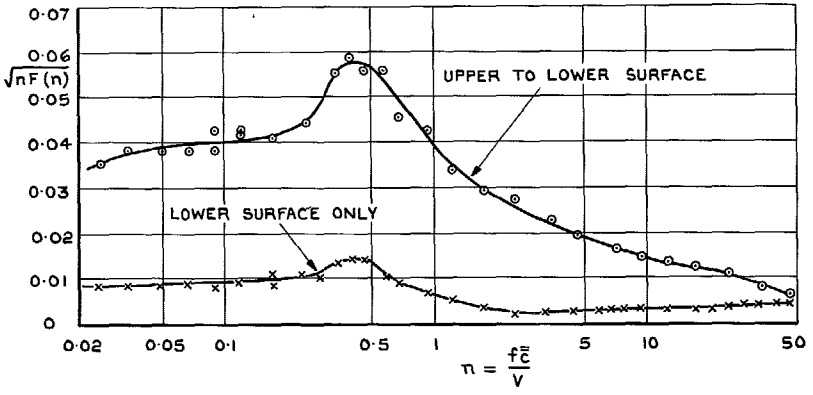

b SPECTRA OF PRESSURE FLUCTUATION $\alpha = 14{\cdot}2°$

FIG. 10 a and b. Comparison of pressure fluctuations on upper and lower surfaces at 0·85c on inner wing. Flaps 0°, no strakes, V = 150 ft/sec.

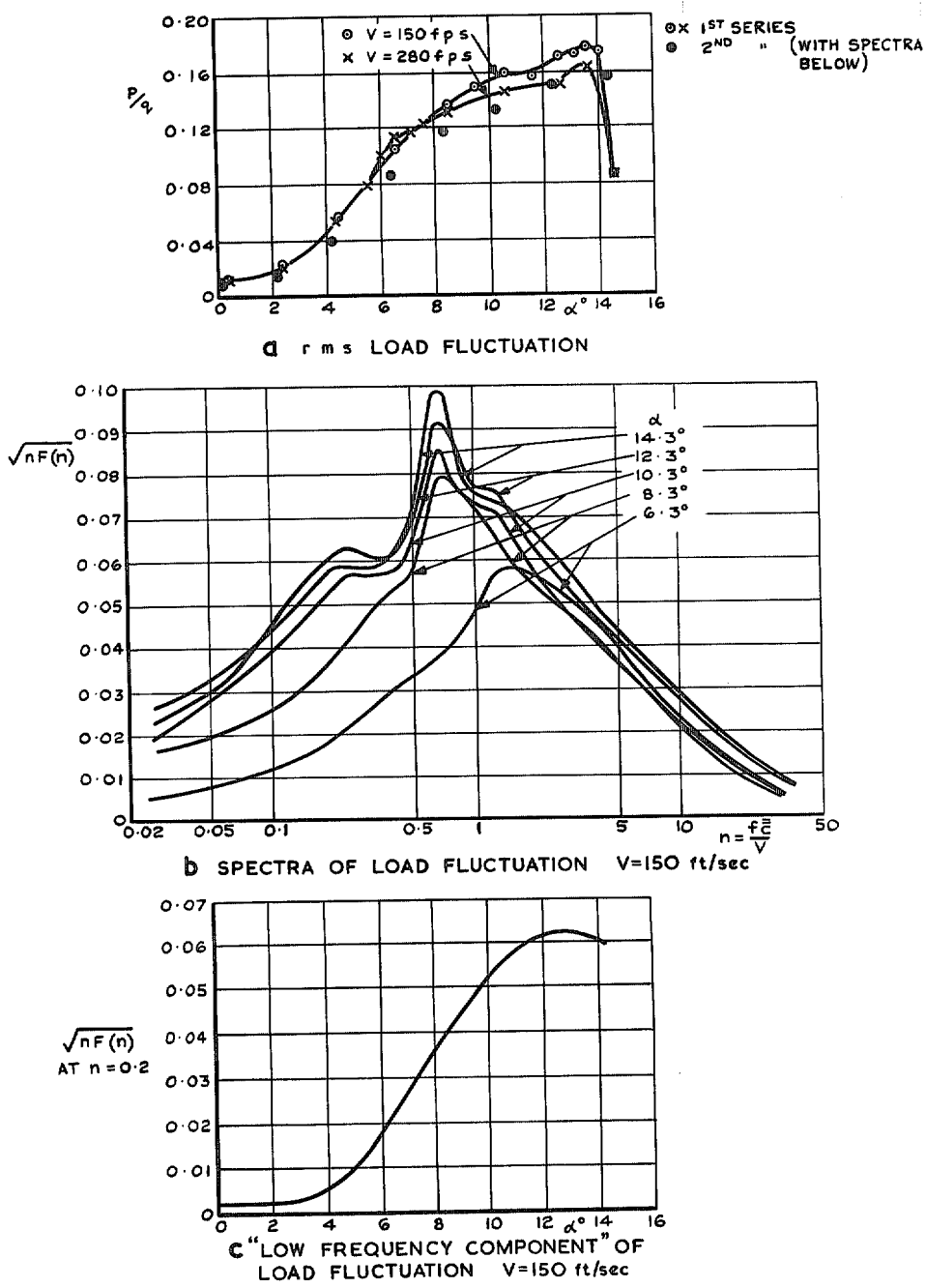

FIG. 11 a – c. Local load fluctuations at 0·5*c* on inner wing. Flaps 50°, no strakes.

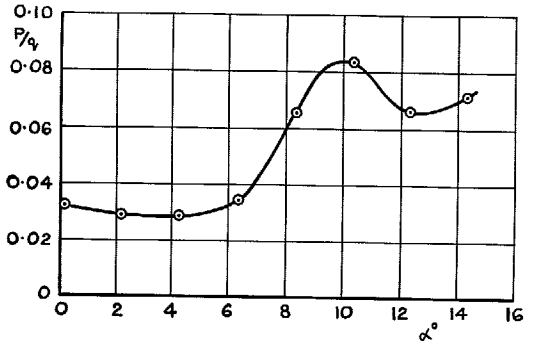

a rms LOAD FLUCTUATION

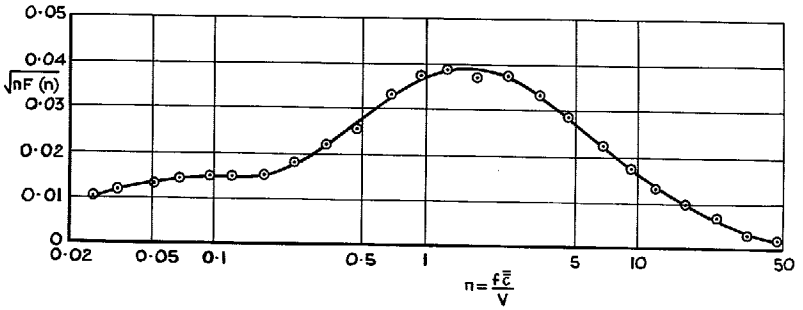

b SPECTRUM OF LOAD FLUCTUATION $\alpha = 12{\cdot}3°$

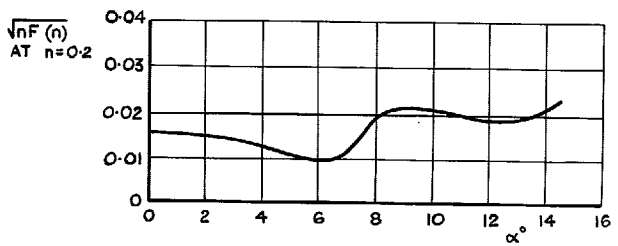

c "LOW FREQUENCY COMPONENT" OF LOAD FLUCTUATION

FIG. 12 a – c. Local load fluctuations at 0·85c on inner wing (i.e. on flap). Flaps 50°, no strakes, V = 150 ft/sec.

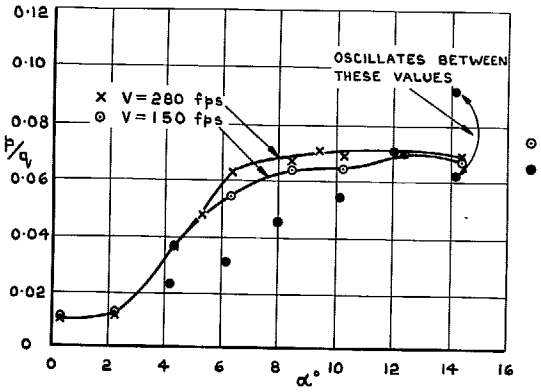

a rms LOAD FLUCTUATION

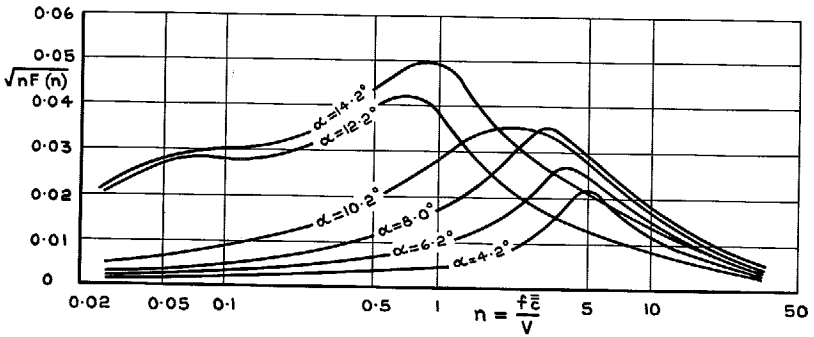

b SPECTRA OF LOAD FLUCTUATION V=150 ft/sec

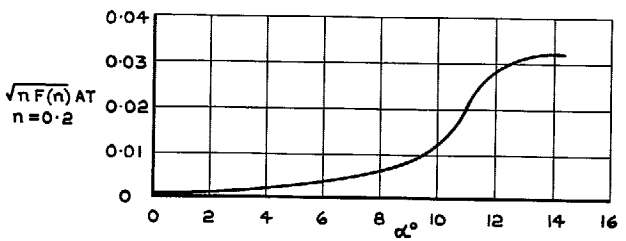

c "LOW FREQUENCY COMPONENT" OF LOAD FLUCTUATION V=150 ft/sec

FIG. 13a – c. Local load fluctuations at 0·5c on inner wing. Flaps 0°, strakes on, V = 150 ft/sec.

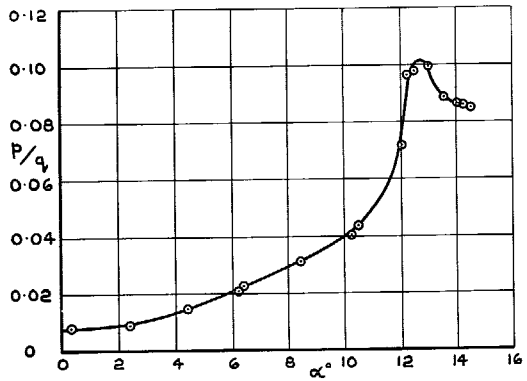

a rms LOAD FLUCTUATION

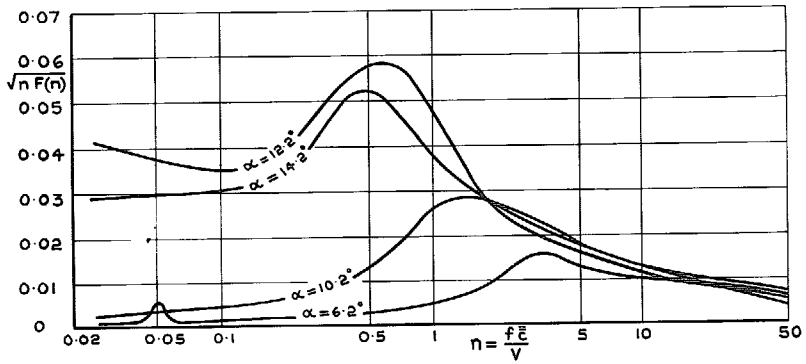

b SPECTRA OF LOAD FLUCTUATION

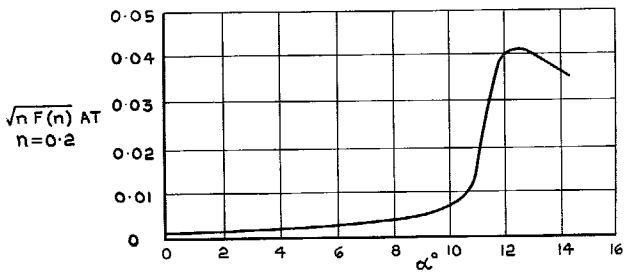

c "LOW FREQUENCY COMPONENT" OF LOAD FLUCTUATION

FIG. 14a – c. Local load fluctuations at 0·85*c* on inner wing. Flaps 0°, strakes on, $V = 150$ ft/sec.

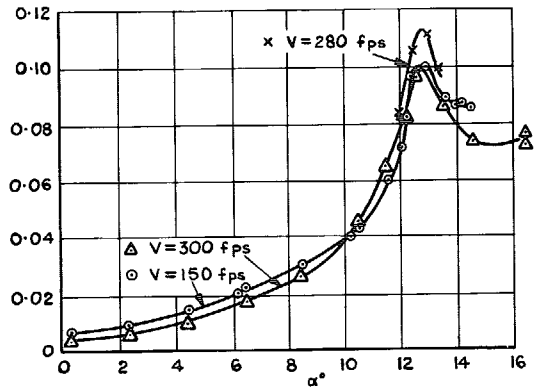

a rms LOAD FLUCTUATION

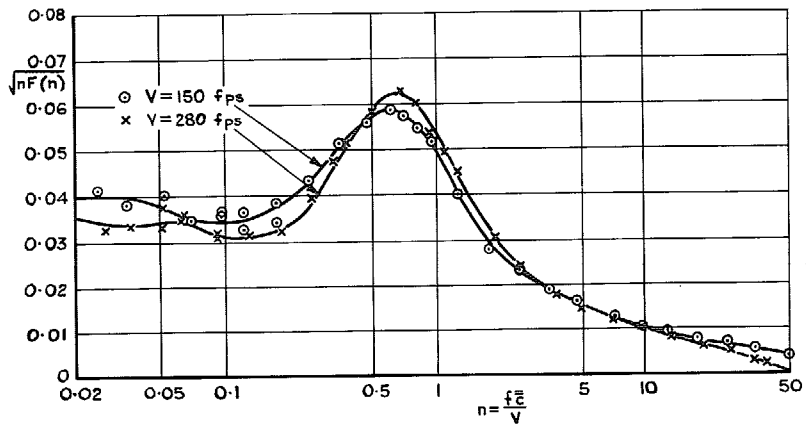

b SPECTRA OF LOAD FLUCTUATION $\alpha = 12{\cdot}2°$

FIG. 15a and b. Effect of wind speed on local load fluctuations at 0·85*c* on inner wing. Flaps 0°, strakes on.

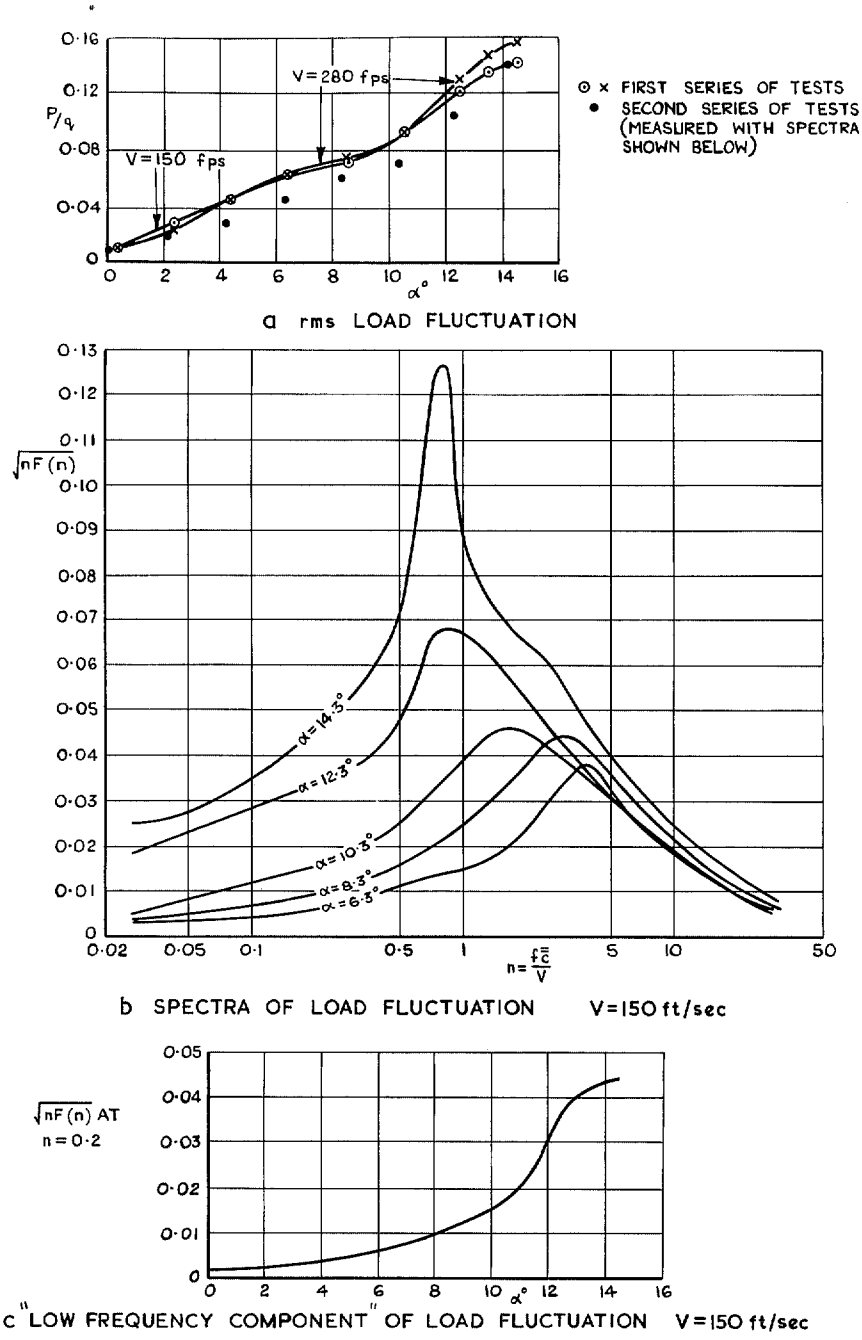

FIG. 16 a – c. Local load fluctuations at 0·5*c* on inner wing. Flaps 50°, strakes on.

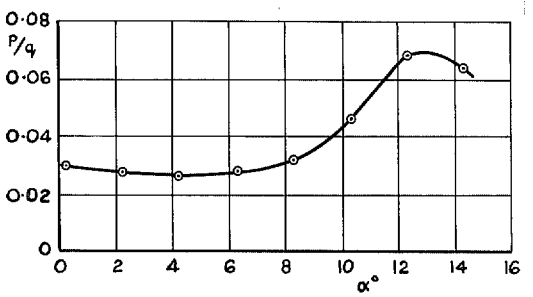

a rms LOAD FLUCTUATION

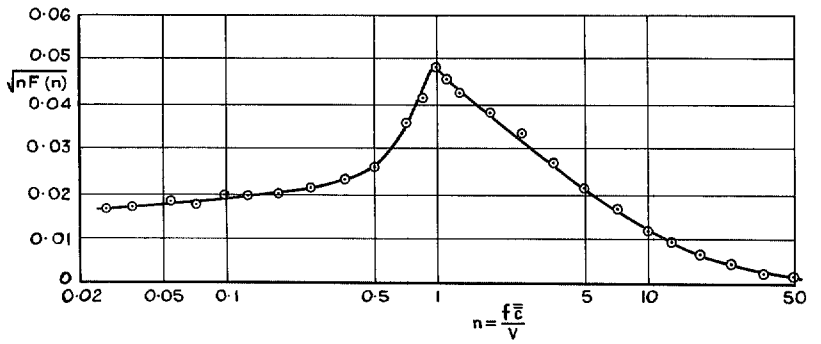

b SPECTRUM OF LOAD FLUCTUATION $\alpha = 12{\cdot}3°$

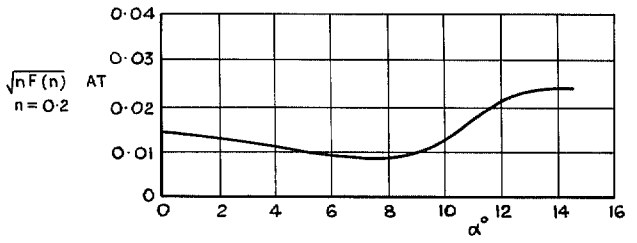

c "LOW FREQUENCY COMPONENT" OF LOAD FLUCTUATION

FIG. 17 a–c. Local load fluctuations at 0·85c on inner wing (i.e. on flap). Flaps 50°, strakes on, $V = 150$ ft/sec.

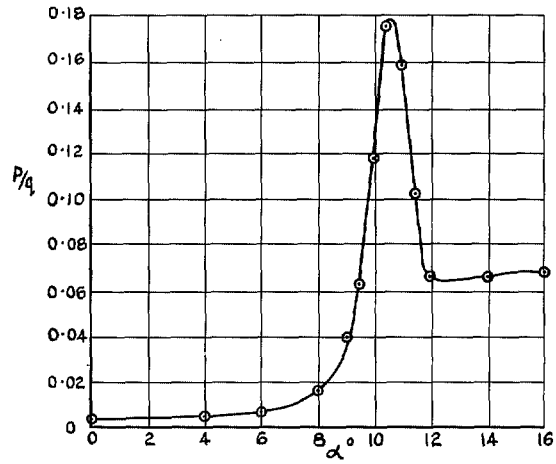

a rms LOAD FLUCTUATION

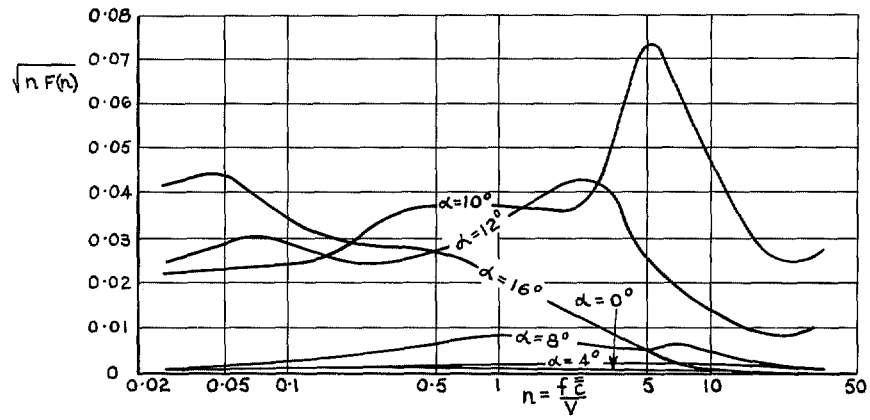

b SPECTRA OF LOAD FLUCTUATION

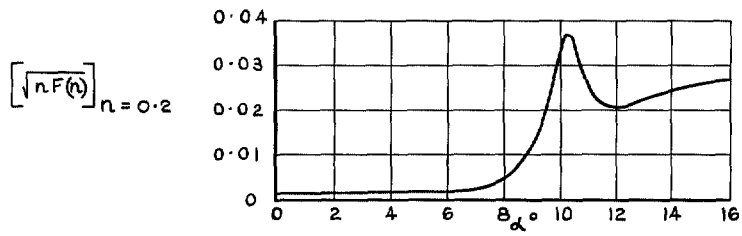

c "LOW FREQUENCY COMPONENT" OF LOAD FLUCTUATION

FIG. 18 a–c. Local load fluctuations at position "A" on outer wing. Flaps 50°, strakes on, $V = 150$ ft/sec.

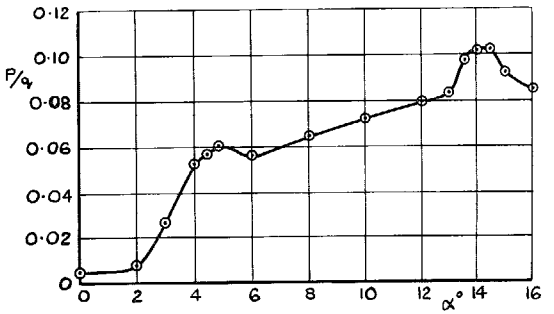

a rms LOAD FLUCTUATION

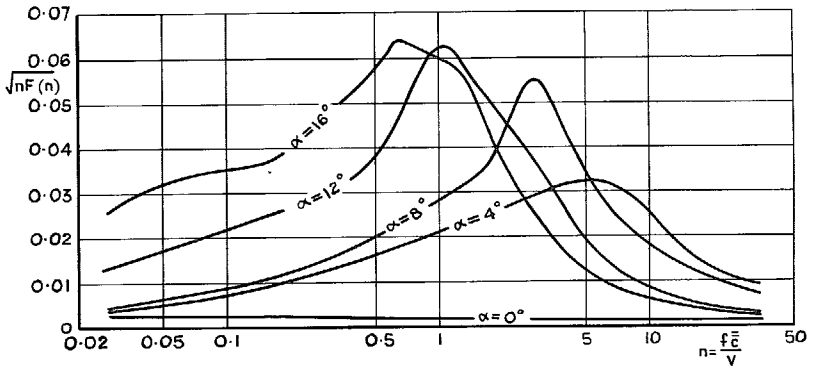

b SPECTRA OF LOAD FLUCTUATION

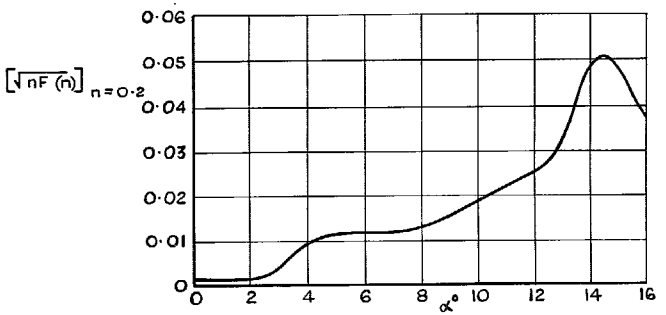

c "LOW FREQUENCY COMPONENT" OF LOAD FLUCTUATION

FIG. 19a–c. Local load fluctuations at position "B" on outer wing. Flaps 50°, strakes on, V = 150 ft/sec.

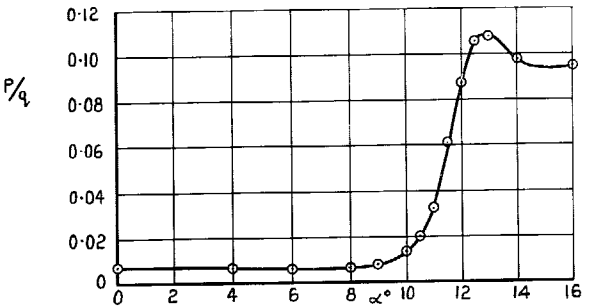

a rms LOAD FLUCTUATION

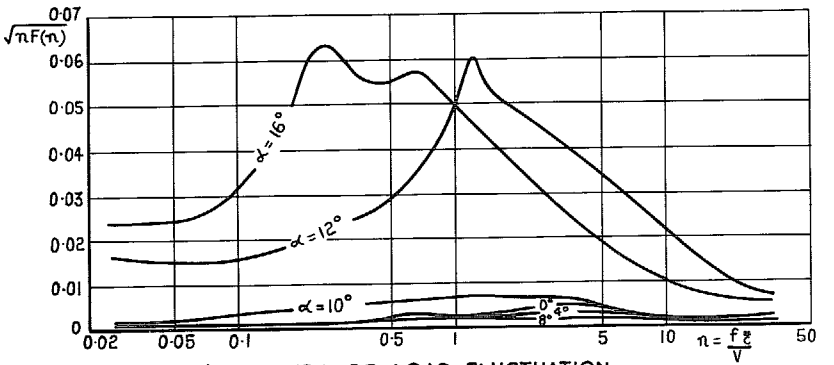

b SPECTRA OF LOAD FLUCTUATION

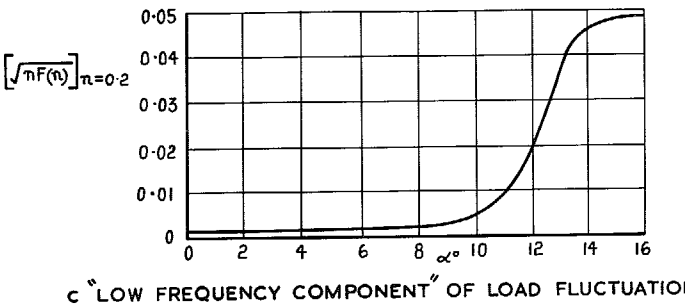

c "LOW FREQUENCY COMPONENT" OF LOAD FLUCTUATION

FIG. 20a–c. Local load fluctuations at position "C" on outer wing. Flaps 50°, strakes on, V = 150 ft/sec.

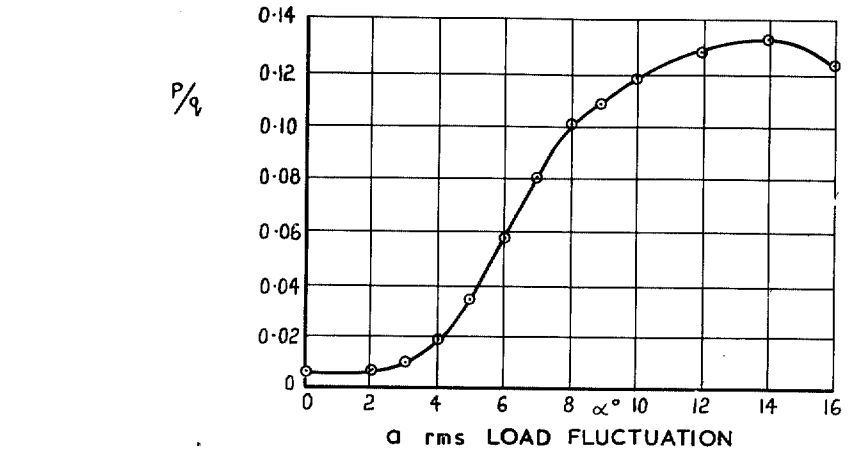

a rms LOAD FLUCTUATION

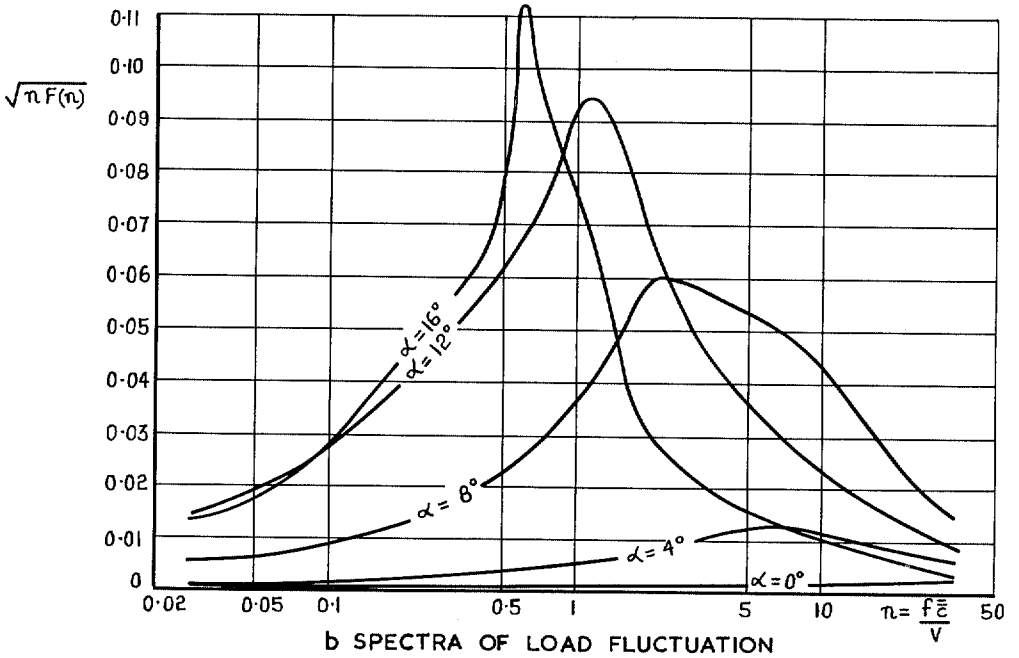

b SPECTRA OF LOAD FLUCTUATION

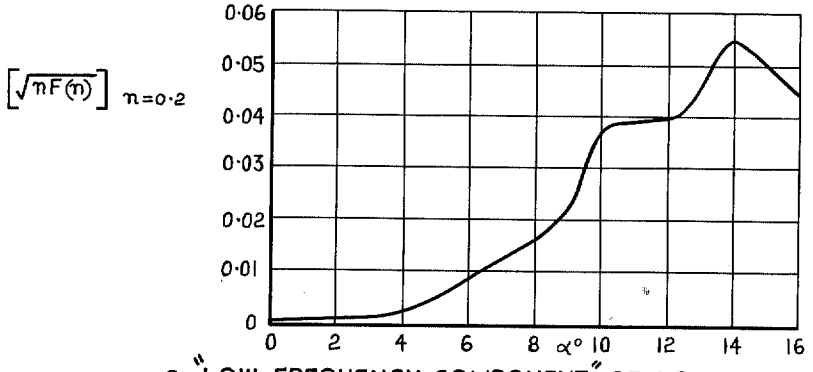

c "LOW FREQUENCY COMPONENT" OF LOAD FLUCTUATION

FIG. 21 a–c. Local load fluctuations at position "D" on outer wing. Flaps 50°, strakes on, $V = 150$ ft/sec.

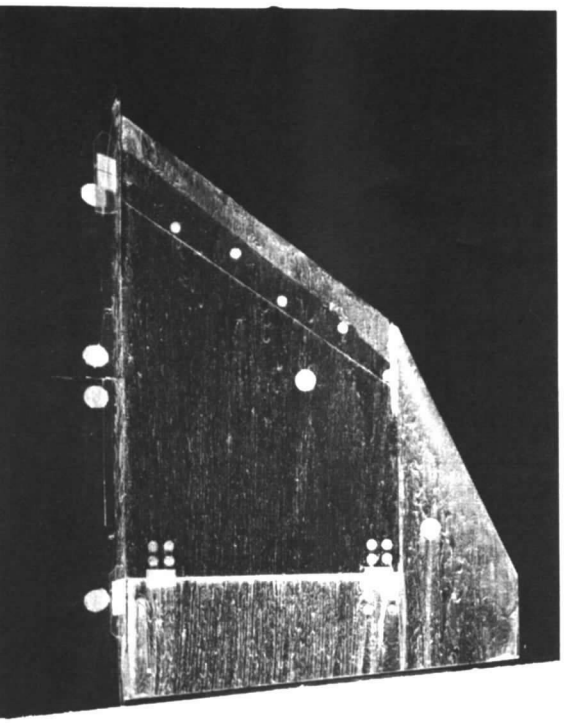

$\alpha = 0°$

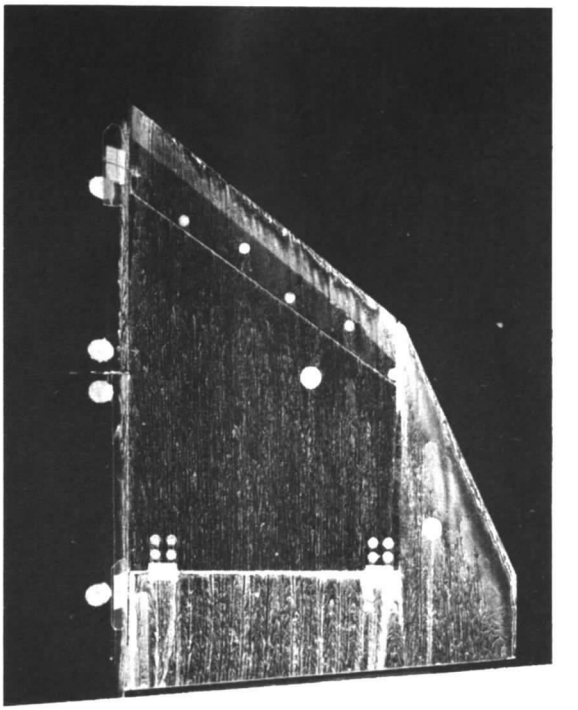

$\alpha = 2°$

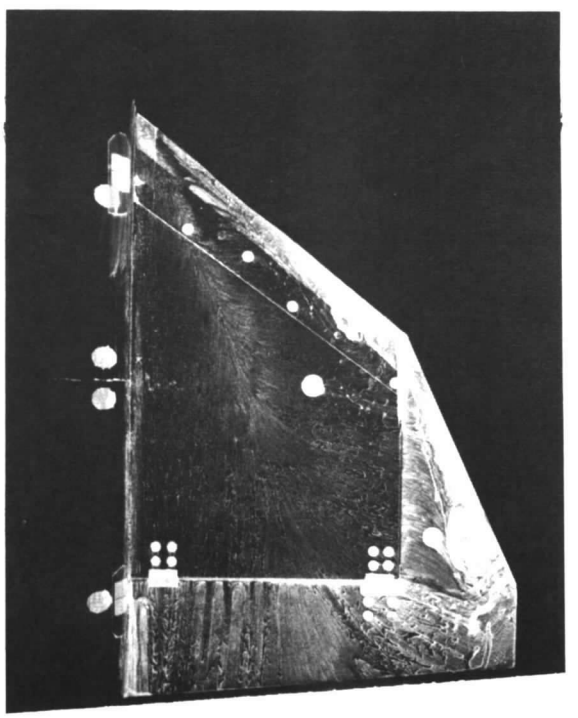

$\alpha = 8°$

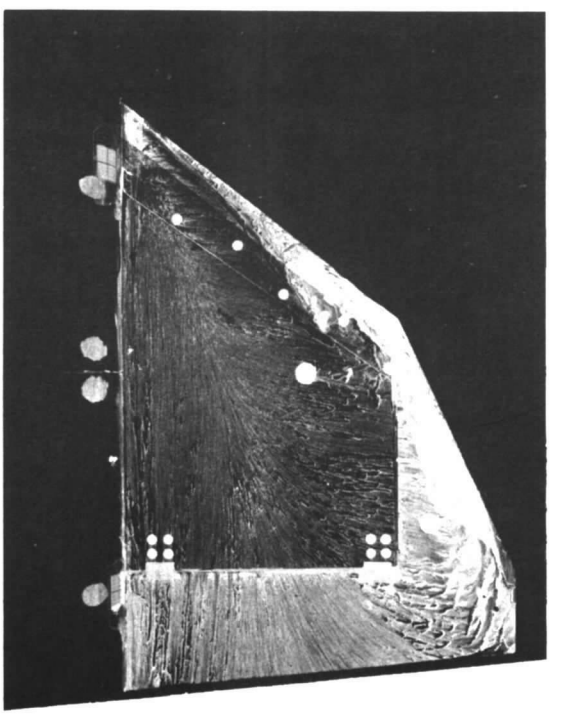

$\alpha = 9°$

FIG. 22. Surface flow patterns on outer wing. Flaps 50°. Strakes on.

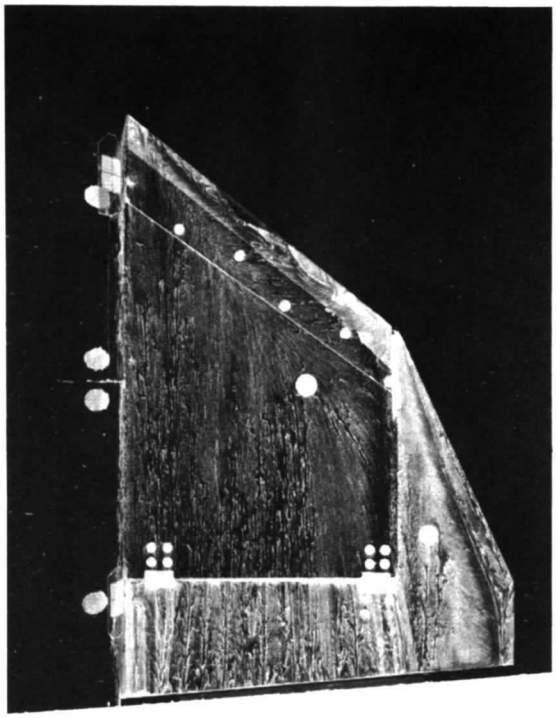

$\alpha = 4°$

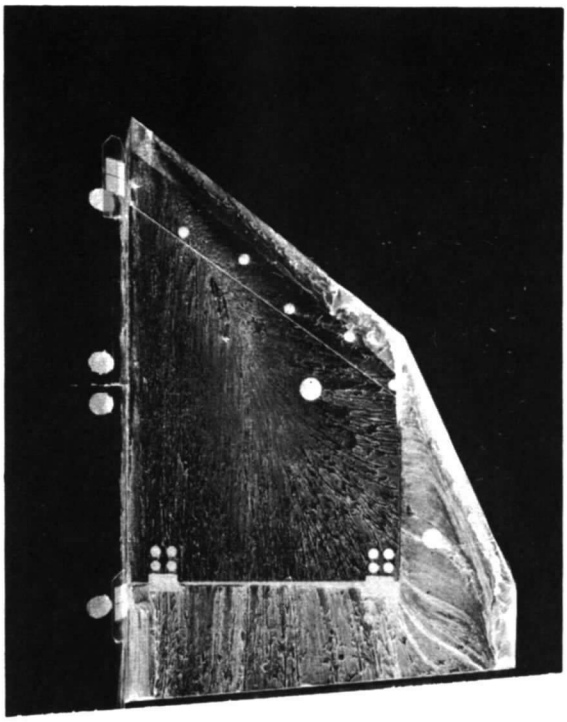

$\alpha = 6°$

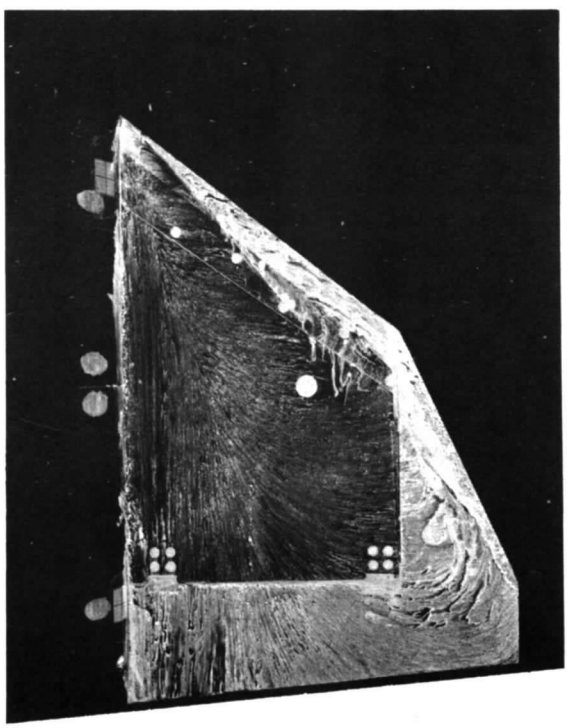

$\alpha = 10°$

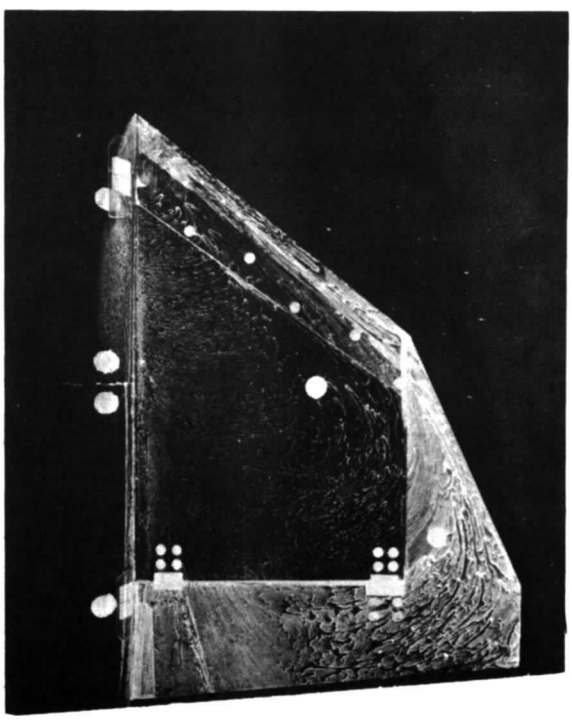

$\alpha = 12°$

FIG. 22 (contd.). Surface flow patterns on outer wing. Flaps 50°. Strakes on.

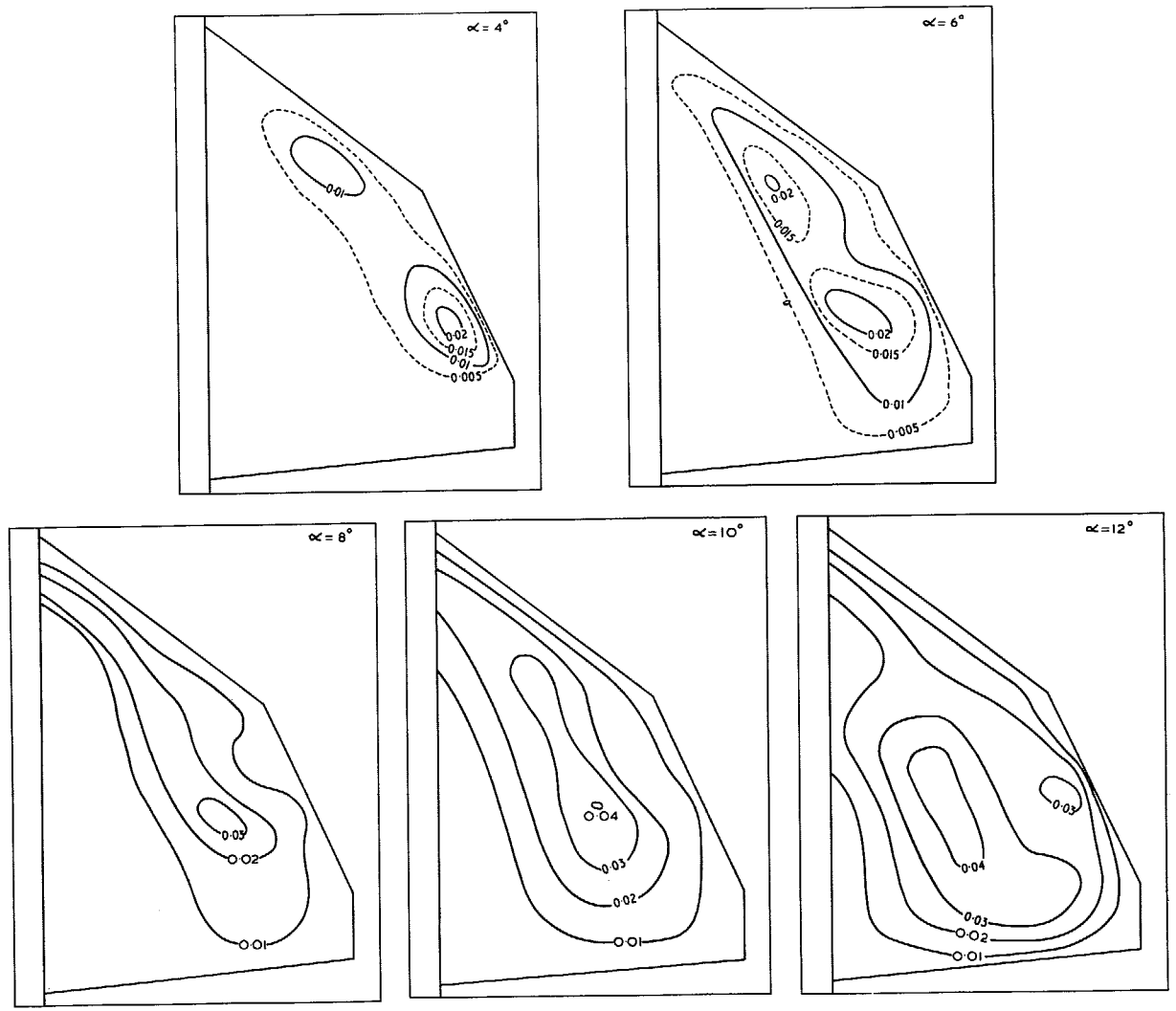

FIG. 23. Contours of "low frequency component" $\left[\sqrt{nF(n)}\right]_{n=0\cdot2}$ of pressure fluctuations on outer wing. Flaps 50°, strakes on, $V = 150$ ft/sec.

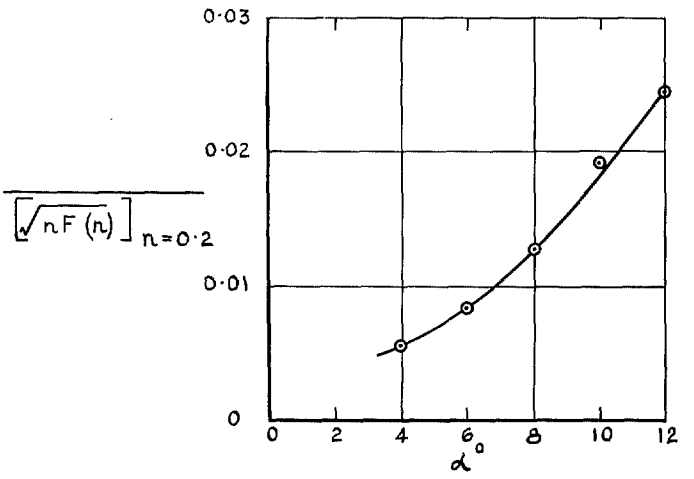

$$\overline{\left[\sqrt{nF(n)}\right]}_{n=0·2} = \sqrt{\frac{\int_0^{A_W}\left[nF(n)\right]_{n=0·2}\,dA}{A_W}}$$

WHERE A IS THE AREA WITHIN THE CONTOUR OF $\left[\sqrt{nF(n)}\right]_{n=0·2}$ AND A_W IS THE AREA OF THE OUTER WING.

FIG. 24. Mean value of "low frequency component" of pressure fluctuation on outer wing. Flaps 50°, strakes on, V = 150 ft/sec.

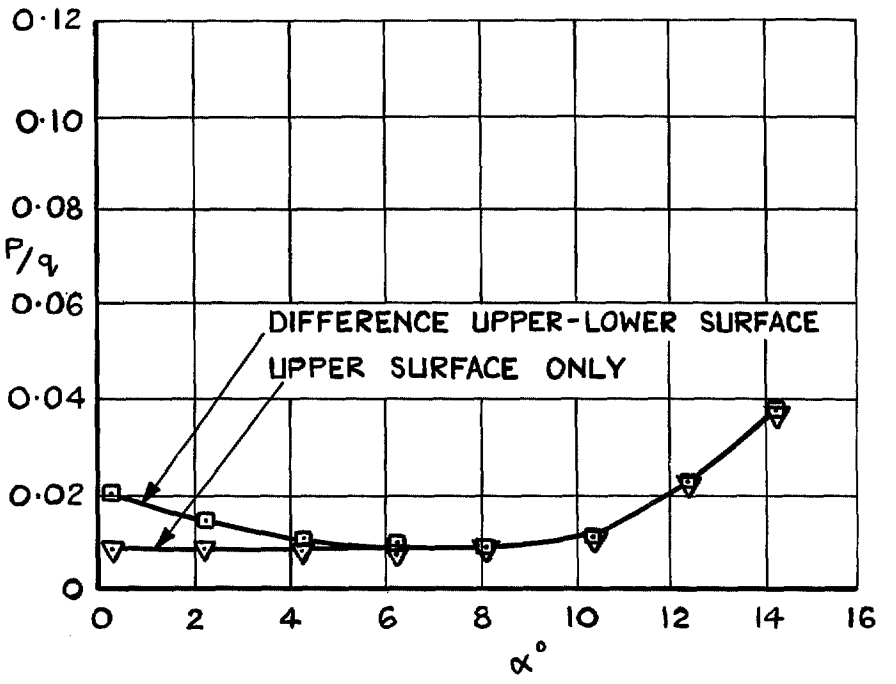

FIG. 25. rms Pressure fluctuations at 0·85c on inner wing with 25° leading edge droop on inner wing. Flaps 0°, no strakes, V = 150 ft/sec.

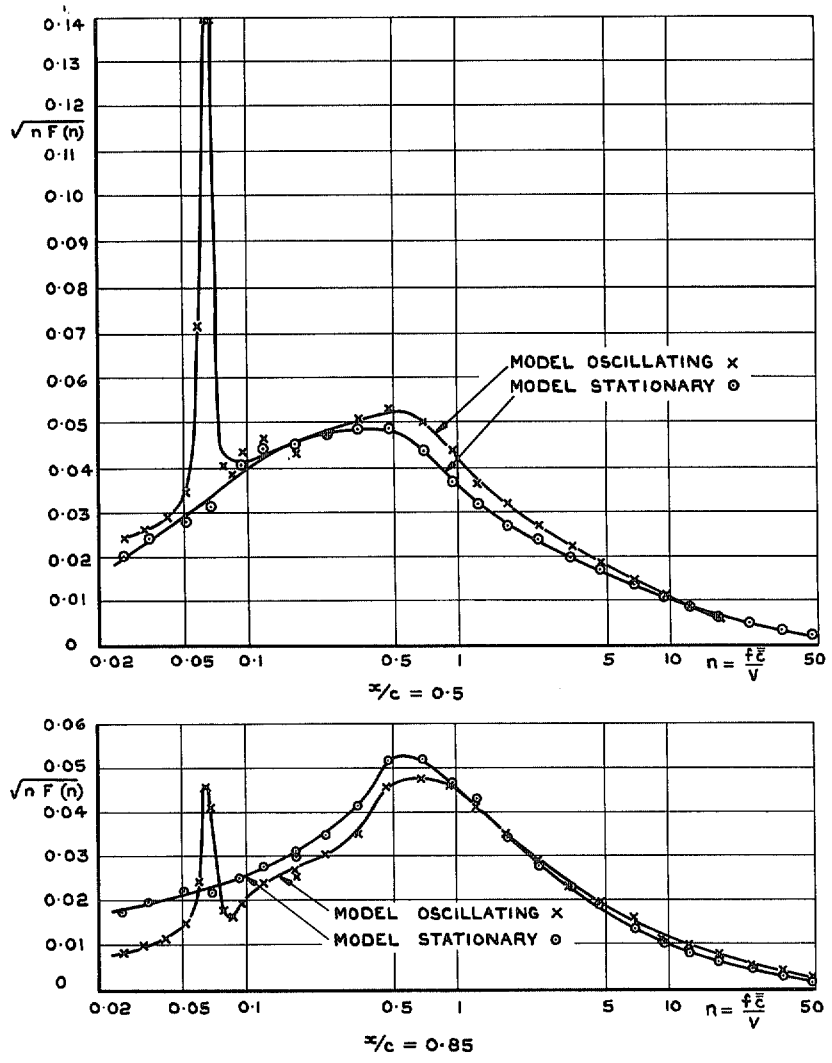

FIG. 26. Effect of oscillation in pitch on spectra of local load fluctuation.
Mean $\alpha = 10{\cdot}1°$ Amplitude of oscillation $= \pm 1°$ Frequency of oscillation $= 7{\cdot}5$ c/sec ($n = 0{\cdot}065$).
Flaps 0°, no strakes, $V = 150$ ft/sec.

Printed in Wales for Her Majesty's Stationery Office by Allens Printers (Wales) Limited

Dd.135646 K 5

© *Crown copyright* 1968

Published by
HER MAJESTY'S STATIONERY OFFICE

To be purchased from
49 High Holborn, London W.C.1
423 Oxford Street, London W.1
13A Castle Street, Edinburgh 2
109 St. Mary Street, Cardiff CF1 1JW
Brazennose Street, Manchester 2
50 Fairfax Street, Bristol BS1 3DE
258–259 Broad Street, Birmingham 1
7–11 Linenhall Street, Belfast BT1 2BA
or through any bookseller

R. & M. No. 3551

S.O. Code No. 23-3551